

Nonlinear Fore(Back)casting and Innovation Filtering for Causal-Noncausal VAR Models

Christian Gourieroux, University of Toronto, Toulouse School of Economics and
CREST^{*},
Joann Jasiak, York University[†]

This version: April 9, 2024

Abstract

We introduce closed-form formulas of out-of-sample predictive densities for forecasting and backcasting of mixed causal-noncausal (Structural) Vector Autoregressive VAR models. These nonlinear and time irreversible non-Gaussian VAR processes are shown to satisfy the Markov property in both calendar and reverse time. A post-estimation inference method for assessing the forecast interval uncertainty due to the preliminary estimation step is introduced too. The nonlinear past-dependent innovations of a mixed causal-noncausal VAR model are defined and their filtering and identification methods are discussed. Our approach is illustrated by a simulation study, and an application to cryptocurrency prices.

Keywords: Predictive Density, Backcasting, Filtering, Nonlinear Innovations, Generalized Covariance (GCov) Estimator, Cryptocurrency Bubble

^{*}e-mail: *Christian.Gourieroux@ensae.fr*

[†]e-mail: *jasiakj@yorku.ca*

The second author acknowledges financial support of the Natural Sciences and Engineering Council of Canada (NSERC)

1 Introduction

There has been a growing interest in applications involving the stationary mixed causal-noncausal Vector Autoregressive (VAR) models and their theoretical properties [Gourieroux, Jasiak (2017),(2022), Davis, Song (2020), Lanne, Luoto (2016),(2021), Swensen (2022), Cubbada, Hecq, Voisin (2023)]. In applied research, the stationary mixed VAR models can replicate local trends, spikes and bubbles characterizing, e.g. the commodity prices and cryptocurrency rates, which are interpreted as non-stationary features in the traditional literature on causal, i.e. past dependent processes. In terms of theoretical properties, the main differences between the mixed VAR's and the traditional causal VAR's are in the assumptions concerning the eigenvalues of the autoregressive matrix coefficients and the errors of the model. More specifically, in the mixed model the roots of the autoregressive characteristic equation can be in modulus either greater or smaller than 1, as opposed to being only greater than 1 in the causal VARs. While the errors of a causal VAR are assumed to be normally distributed, the errors of a mixed VAR need to be non-Gaussian for the identification of causal and noncausal dynamics. Thus, the traditional Gaussian Maximum Likelihood (ML) and Least Squares estimators are flawed in applications to mixed VAR's. Under parametric distributional assumptions, the ML estimators based on non-Gaussian likelihood functions can be used for the mixed VAR models, as shown in Davis, Song (2020). When the error distribution is left unspecified, the Generalized Covariance (GCov) estimator is available, providing consistent, asymptotically normally distributed and semi-parametrically efficient parameters estimates in one step [Gourieroux, Jasiak (2023)].

There is an important difference between the errors of causal and mixed VAR models, other than non-Gaussianity. Unlike the errors of causal VARs, those of mixed VAR's are not uncorrelated / independent from the past values of the process. Hence, they cannot be interpreted as innovations. For this reason, innovation-based inference, such as impulse response analysis (IRF) and forecast error variance decomposition (FEVD) routinely conducted in the causal VAR models cannot be applied in the same way to the mixed VAR models³. It has to account for the nonlinear dynamic features of the mixed VAR model. So far, the nonlinear causal innovations of a mixed VAR model have not been defined in the literature.

Another difficulty arises with the fore- and backcasting of the mixed VAR models. A mixed VAR model with non-Gaussian errors cannot be forecast from its conditional expectation only, unlike the traditional causal VAR model. For out-of-sample (oos) nonlinear forecasting of mixed causal-noncausal VAR processes, there exist in the literature a simulation-based method of forecasting given in Nyberg, Saikkonen (2014) and a Bayesian method in Lanne, Luoto (2016), which are valid for a constraint multiplicative mixed VAR representation. An operational causal predictive density

³See, e.g. Lutkepohl (1990).

in closed-form for the multivariate mixed VAR models has been deemed infeasible in Fries, Zakoian (2019) ⁴.

Moreover, the backcasting, which is straightforward for the time reversible linear Gaussian causal VAR processes, is complicated in this context as well. The mixed VAR does not satisfy the assumption of Gaussianity ensuring the time reversibility, which underlies the commonly used time series and machine learning methods of backcasting [Twumasi, Twumasi (2022)]. A closed-form formula of nonlinear backcasting for mixed VAR models has not been introduced in the literature yet.

This paper addresses the two problems of i) the lack of closed-form predictive densities for forecasting and backcasting and ii) the lack of a definition of nonlinear causal innovations for the mixed VAR model and their use for nonlinear impulse response analysis.

We provide closed-form formulas of backward and forward predictive density for out of sample forecasting and backcasting of mixed causal-noncausal VAR processes. For fore(back)casting, we show that the mixed VAR is a nonlinear Markov process in both calendar and reverse time while being time-irreversible. The closed-form expression of predictive densities for fore- and backcasting the mixed causal-noncausal VAR processes are given at horizon 1. They can be used sequentially to predict at any horizon.

From the predictive densities, we infer the point forecasts and prediction intervals. A post-estimation inference method for assessing the forecast interval uncertainty due to the preliminary estimation step is introduced too. A confidence set of the predicted set is proposed as a post-estimation inference method to capture the effect of the preliminary estimation step on the prediction interval.

The nonlinear causal innovations are defined by extending the results in Koop, Pesaran, Potter (1996), Potter (2000), and Gouriéroux, Jasiak (2005). We determine their relationship with the model errors and discuss their identification and in-sample filtering.

The forecast performance and the nonlinear causal innovations analysis are illustrated by simulations and empirical applications. We use the one-step semi-parametric GCov estimators introduced in Gouriéroux, Jasiak (2023) for VAR models. This approach does not require any distributional assumptions on the errors of the model, except for their non-Gaussianity. The semi-parametric estimation method distinguishes our approach from the existing literature employing maximum likelihood-based methods [Andrews et al. (2006), Davis, Song (2020), Swensen (2022)], which are consistent provided that the distributional assumptions are satisfied.

The paper is organized as follows. Section 2 describes the causal-noncausal VAR model and its constrained multiplicative form. Section 3 recalls the state-space representation of the mixed VAR

⁴"The predictive density is generally not available under closed form", Fries, Zakoian (2019)

model and derives the closed-form formulas of the multivariate predictive density for forecasting and backcasting. Section 4 defines the nonlinear causal innovations and discusses their identification and filtering. Section 5 reviews the semi-parametric estimation of the mixed VAR model and introduces a filtering algorithm and post-estimation inference on the random prediction set. A simulation study and an empirical application to a bivariate process of Bitcoin/USD and Ethereum/USD exchange rates are provided in Section 6. Section 7 concludes. The technical results are given in Appendices A.1-A.3. Appendix A.1 contains the proof of the forward and backward predictive density formula. Appendix A.2 explains the constraints induced by the multiplicative representation of a causal-noncausal VAR model. Online Appendix A.3 examines the (under)-identification of nonlinear innovations in a multivariate framework.

Additional information is provided in the online Appendices B, C and D, which include a discussion of the identification conditions for Independent Component Analysis (ICA), the closed-form expression of the kernel-based semi-nonparametric estimator of predictive density, and additional results for the empirical applications.

2 Mixed Causal-Noncausal Processes

This Section reviews the causal-noncausal VAR(p) model studied in Gouriéroux, Jasiak (2017), Davis, Song (2020)⁵, and Swensen (2022).

2.1 The Model

The multivariate causal-noncausal VAR(p), referred to as the mixed VAR process henceforth, is defined by:

$$Y_t = \Phi_1 Y_{t-1} + \cdots + \Phi_p Y_{t-p} + \varepsilon_t, \quad (2.1)$$

where Y_t is a vector of size m , Φ_j , $j = 1, \dots, p$ are matrices of autoregressive coefficients of dimension $m \times m$ and (ε_t) is a sequence of errors, which are serially independent, identically distributed (i.i.d.) random vectors of dimension m with mean zero and finite variance-covariance matrix Σ . Errors (ε_t) are assumed to have a non-Gaussian distribution. Since (ε_t) is not assumed independent of past Y 's, this error process cannot be interpreted as an innovation process.

We assume that the roots of the characteristic equation of the autoregressive polynomial matrix $\det(Id - \Phi_1 \lambda - \cdots - \Phi_p \lambda^p) = 0$ are of modulus either strictly greater, or strictly less than one, i.e. are either outside, or inside the unit circle. Then, there exists a unique strictly stationary solution to the VAR model (2.1).

⁵based on a working paper from 2012.

The strictly stationary solution (Y_t) to model (2.1) can be written as a two-sided moving average in errors ε_t :

$$Y_t = \sum_{j=-\infty}^{+\infty} C_j \varepsilon_{t-j}. \quad (2.2)$$

This is a linear time series, according to the terminology of Rosenblatt (2012). The matrices of coefficients on the past and future terms of this MA representation are uniquely defined when ε_t is non-Gaussian, which is an identifying assumption. Process Y_t is said to be causal in ε_t , if $Y_t = \sum_{j=0}^{+\infty} C_j \varepsilon_{t-j}$, noncausal in ε_t , if $Y_t = \sum_{j=-\infty}^{-1} C_j \varepsilon_{t-j} = \sum_{j=1}^{+\infty} C_{-j} \varepsilon_{t+j}$, or mixed, otherwise.

In the presence of a noncausal component, the assumption of strict stationarity of (Y_t) implies the nonlinear causal dynamics of Y_t with past-dependent conditional heteroscedasticity. Then, the process (Y_t) can be characterized by a possibly complicated conditional distribution of Y_{t+h} given $\underline{Y}_t = (Y_t, Y_{t-1}, \dots)$ for $h = 1, 2, \dots$, that provides nonlinear out-of-sample (oos) predictions.

A process (Y_t) with nonlinear causal dynamics may display local trends, spikes and bubbles similar to those observed in the time series of commodity (oil) prices, exchange rates, or cryptocurrency prices [Gourieroux, Zakoian (2017), Gourieroux, Jasiak (2017), Gourieroux, Jasiak, Tong (2021)].

2.2 Multiplicative VAR

A constrained multiplicative Mixed Autoregressive (MAR) representation of the mixed VAR model was proposed by Lanne, Saikkonen (2013): $\Phi(L)\Psi(L^{-1})Y_t = \varepsilon_t^*$, where the matrices of autoregressive polynomials Φ and Ψ have both roots outside the unit circle and ε_t^* is an i.i.d. sequence of errors. Davis, Song (2020), Swensen (2022), point out that the multiplicative representation of a mixed causal-noncausal VAR model does not always exist and Cubbada, Hecq, Voisin (2022) note that it is not equivalent to $\Psi(L^{-1})\Phi(L)Y_t = \varepsilon_t^*$, since $\Psi(L^{-1})$ and $\Phi(L)$ do not commute, in general. More precisely, the multiplicative representation exists for the univariate mixed processes [Breidt et al. (1991), Lanne, Saikkonen (2008)] and for the multivariate mixed VAR(1) process [Gourieroux, Jasiak (2017), Corollary 3 and Section 5]. Otherwise, Appendix A.2 shows that the multiplicative representation may not be compatible with the representation (2.1) of the VAR model. For example, the multiplicative VAR(2) model $(Id - \Phi L)(Id - \Psi L^{-1})Y_t = \varepsilon_t^*$ where the matrix polynomials have roots of modulus strictly greater than 1 and (ε_t^*) are i.i.d., can be written under the form $Y_t = \Phi_1 Y_{t-1} + \Phi_2 Y_{t-2} + \varepsilon_t$. However, the errors ε_t are independent only if the matrix Ψ is invertible.

The set of multiplicative VAR and mixed VAR models are non-nested, i.e. a mixed model does not always admit a multiplicative form and a multiplicative VAR model cannot always be written as a mixed VAR. We focus our attention on the mixed VAR model in this paper.

3 State-Space Representation and Predictive Density

Let us recall the state-space representation of the mixed VAR process.

3.1 State-Space Representation

We consider a mixed VAR(p) process of dimension m :

$$Y_t = \Phi_1 Y_{t-1} + \cdots + \Phi_p Y_{t-p} + \varepsilon_t, \quad (3.1)$$

where the serially i.i.d. error vectors ε_t have a continuous joint distribution with probability density function g . These parameters are assumed given in this Section. We assume that the roots of:

$$\det(Id - \Phi_1 z - \cdots - \Phi_p z^p) = 0, \quad (3.2)$$

are not on the unit circle. Then, there exists a unique stationary solution of model (3.1) with a two-sided moving average representation in (ε_t) .

a) *The mixed VAR(1) representation of a mixed VAR(p) process*

As it is commonly done in the literature on multivariate causal autoregressive processes, model (3.1) can be rewritten as a $n = mp$ multivariate mixed VAR(1) model, by stacking the present and lagged values of process (Y_t) :

$$\begin{pmatrix} Y_t \\ \tilde{Y}_{t-1} \end{pmatrix} \equiv \begin{pmatrix} Y_t \\ Y_{t-1} \\ \vdots \\ Y_{t-p+1} \end{pmatrix} = \Psi \begin{pmatrix} Y_{t-1} \\ \tilde{Y}_{t-2} \end{pmatrix} + \begin{pmatrix} \varepsilon_t \\ 0 \end{pmatrix}, \quad (3.3)$$

with

$$\Psi = \begin{pmatrix} \Phi_1 & \cdots & \cdots & \Phi_p \\ Id & 0 & \cdots & \\ \vdots & \ddots & \ddots & \vdots \\ 0 & \cdots & Id & 0 \end{pmatrix}. \quad (3.4)$$

The eigenvalues of the autoregressive matrix Ψ are the reciprocals of the roots of the characteristic equation (3.2).

b) *The Change of Basis*

Matrix Ψ has a real Jordan representation: $\Psi = A \begin{pmatrix} J_1 & 0 \\ 0 & J_2 \end{pmatrix} A^{-1}$, where J_1 (resp. J_2) are real $(n_1 \times n_1)$ (resp. $(n_2 \times n_2)$) matrices where $n_2 = n - n_1$ with all eigenvalues of modulus strictly less than 1 [resp. strictly larger than 1] and A is a $(n \times n)$ invertible matrix [see Perko (2001), Gouriéroux,

Jasiak (2016), Section 5.2, Davis, Song (2020), Remark 2.1. for real Jordan representations]. Then, equation (3.3) can be rewritten after the change of basis A^{-1} as:

$$A^{-1} \begin{pmatrix} Y_t \\ \tilde{Y}_{t-1} \end{pmatrix} = \begin{pmatrix} J_1 & 0 \\ 0 & J_2 \end{pmatrix} A^{-1} \begin{pmatrix} Y_{t-1} \\ \tilde{Y}_{t-2} \end{pmatrix} + A^{-1} \begin{pmatrix} \varepsilon_t \\ 0 \end{pmatrix}. \quad (3.5)$$

Let us introduce a block decomposition of A^{-1} :

$$A^{-1} \equiv \begin{pmatrix} A^1 \\ A^2 \end{pmatrix}, \quad (3.6)$$

where A^1 is of dimension $(n_1 \times n)$ and the transformed variables:

$$Z_t = \begin{pmatrix} Z_{1,t} \\ Z_{2,t} \end{pmatrix} = A^{-1} \begin{pmatrix} Y_t \\ \tilde{Y}_{t-1} \end{pmatrix}, \quad \eta_t = \begin{pmatrix} \eta_{1,t} \\ \eta_{2,t} \end{pmatrix} = A^{-1} \begin{pmatrix} \varepsilon_t \\ 0 \end{pmatrix}. \quad (3.7)$$

Then, we get two sets of state components of process (Y_t) such that:

$$\begin{aligned} Z_{1,t} &= J_1 Z_{1,t-1} + \eta_{1,t}, \\ Z_{2,t} &= J_2 Z_{2,t-1} + \eta_{2,t}. \end{aligned} \quad (3.8)$$

The state-space representation of process (Y_t) consists of:

state equations of state variables Z_t that follow the causal and non-causal equations (3.8);

measurement equations obtained by solving for Y_t from: $\begin{pmatrix} Y_t \\ \tilde{Y}_{t-1} \end{pmatrix} = AZ_t$.

These measurement equations are deterministic and the filtrations generated by (Y_t) and (Z_t) are identical.

Since the Jordan representation is not unique, the state-space representation is not unique either. It depends on the choice of state variables, i.e. the latent factors Z_1 and Z_2 , up to linear invertible transformations.

c) State Linear Innovations

The first set of state equations (3.8) defines the causal VAR(1) process $(Z_{1,t})$. Thus, the process $(Z_{1,t})$ has the causal MA(∞) representation:

$$Z_{1,t} = \sum_{j=0}^{+\infty} J_1^j \eta_{1,t-j}, \quad (3.9)$$

with $\eta_{1,t}$ as a function of $\varepsilon_t, \varepsilon_{t-1}, \dots$

The second set of state equations (3.8) needs to be inverted to obtain a MA representation in matrices with eigenvalues of modulus strictly less than 1. We get:

$$Z_{2,t} = J_2^{-1} Z_{2,t+1} - J_2^{-1} \eta_{2,t+1}, = - \sum_{j=0}^{+\infty} [J_2^{-j-1} \eta_{2,t+j+1}]. \quad (3.10)$$

Therefore, $(Z_{2,t})$ is a noncausal process with a one-sided moving average representation in future values $\varepsilon_{t+1}, \varepsilon_{t+2}, \dots$.

Let us now discuss the state-specific linear innovations $\eta_{1,t}, \eta_{2,t}$. From equations (3.9), (3.10) and the stationarity conditions, it follows that:

$$\eta_{1,t} = Z_{1,t} - E(Z_{1,t} | \underline{Z}_{1,t-1}), \quad \eta_{2,t} = Z_{2,t} - E(Z_{2,t} | \bar{Z}_{2,t+1}), \quad (3.11)$$

where $\underline{Z}_{1,t-1} = Z_{1,t-1}, Z_{1,t-2}, \dots$ and $\bar{Z}_{2,t+1} = Z_{2,t+1}, Z_{2,t+2}, \dots$. Therefore, $\eta_{1,t}$ (resp. $\eta_{2,t}$) can be interpreted as the causal linear innovations of $Z_{1,t}$ based on the information $\underline{Z}_{1,t-1}$ (resp. noncausal linear innovation of $Z_{2,t}$ based on the information $\bar{Z}_{2,t+1}$). It is important to note that the information set $\underline{Z}_{1,t-1}$ (resp. $\bar{Z}_{2,t+1}$) differs in general from the global causal information set $\underline{Y}_{t-1} = \underline{Z}_{t-1}$ (resp. $\bar{Y}_{t+1} = \bar{Z}_{t+1}$). Later, in Section 4, we clarify this interpretation by introducing the notion of a nonlinear innovation that takes into account all available information. To do that we need first to derive the expressions of forward and backward predictive densities.

3.2 Out-of-Sample Predictive Density

The expression of the predictive density of Y_{T+1} given $\underline{Y}_T = (Y_T, Y_{T-1}, \dots)$ is given below and derived in Appendix A.1. This expression is written for given Φ_1, Φ_2, \dots and joint error density g .

Proposition 1: The conditional probability density function (pdf) of Y_{T+1} given \underline{Y}_T is:

$$l(y | \underline{Y}_T) = \frac{l_2 \left[A^2 \begin{pmatrix} y \\ \tilde{Y}_T \end{pmatrix} \right]}{l_2 \left[A^2 \begin{pmatrix} Y_T \\ \tilde{Y}_{T-1} \end{pmatrix} \right]} |\det J_2| g(y - \Phi_1 Y_T - \dots - \Phi_p Y_{T-p+1}), \quad (3.12)$$

where $l_2(z_2)$ is the stationary pdf of $Z_{2,t} = A^2 \begin{pmatrix} Y_t \\ \tilde{Y}_{t-1} \end{pmatrix}$, if $n_2 \geq 1$. In the pure noncausal process, $n_2 = 0$, we have $l(y | \underline{Y}_T) = g(y - \Phi_1 Y_T - \dots - \Phi_p Y_{T-p+1})$.

In the special case of the mixed VAR(1) process with $p = 1$, the predictive density becomes:

$$l(y | \underline{Y}_T) = l(y | Y_T) = \frac{l_2(A^2 y)}{l_2(A^2 Y_T)} |\det J_2| g(y - \Phi Y_T). \quad (3.13)$$

Proof: See Appendix A.1.

This predictive density is constrained by the VAR representation (3.1). It is a semi-parametric function of parameters Φ_1, \dots, Φ_p , determining A^2 and J_2 , and of functional parameters g, l_2 . Except

if the distribution is multivariate Gaussian, the predictive density has a complicated form, with several modes and a conditional mean which is not linear in \underline{Y}_{t-1} , in general. From equation (3.12) and the deterministic relation between Y_t and Z_t , it follows that:

Corollary 1: Markov Property

The mixed VAR(p) process (Y_t) [resp. the state process (Z_t)] is a Markov processes of order p [resp. of order 1] in calendar time for $n_2 \geq 1$. They are both Markov in reverse time too.

This corollary extends to linear mixed causal-noncausal processes of any autoregressive order, the result of Cambanis, Fakhre-Zakeri (1994), who show that a linear pure noncausal autoregressive process of order 1 is a causal Markov process of order 1.

3.3 Backward Predictive Density

Since the mixed VAR process of order p is Markov of order p both in calendar and reverse time, we can derive the closed-form expression of the backward predictive density in reverse time for backcasting.

Corollary 2: Backcasting

In a mixed VAR(1) model the backward predictive density of Y_{T-1} given Y_T is:

$$l_B(y|Y_T) = \frac{l_1(A^1 y)}{l_1(A^1 y_T)} |det J_2| g(Y_T - \Phi y),$$

where l_1 is the stationary density of Z_{1t} and g is the density of ε .

Proof: See Appendix A.1.

3.4 Discussion

By considering jointly Proposition 1 and Corollary 2, we can see that the mixed VAR models have a nonlinear dynamic structure that allows for extending to nonlinear framework the standard Kalman filter for linear Gaussian processes.

We observe that there exists a multiplicity of real Jordan representations and of matrices A built from extended real eigenspaces (in the presence of complex conjugate eigenvalues). However, $\det J_2 = \prod_{j=1}^{n_2} \lambda_j$, where $|\lambda_j| > 1$, $j = 1, \dots, n_2$, is independent of the real Jordan representation. Similarly, the noncausal component Z_2 is defined up to a linear invertible transformation. Since

the Jacobian is the same for the numerator and denominator of the ratio $\frac{l_2 \left[A^2 \begin{pmatrix} y \\ \tilde{Y}_T \end{pmatrix} \right]}{l_2 \left[A^2 \begin{pmatrix} Y_T \\ \tilde{Y}_{T-1} \end{pmatrix} \right]}$, it has

no effect on the ratio. Thus, the expression of $l(y|\underline{Y}_T)$ does not depend on the selected real Jordan representation, that is on the selected state-space representation.

A mixed VAR process has nonlinear causal dynamics, which is captured by the predictive density. For this nonlinear and non-Gaussian process, the predictive density provides the oos prediction intervals at various horizons, and replaces the linear pointwise predictions and prediction intervals of causal VARs.

The closed-form expression of the predictive density is available at horizon 1. It can be written at horizon h as a multivariate integral over h future values of the process. For given Φ_1, \dots, Φ_p and g , the predictive density at horizon h can be approximated as follows: The closed-form predictive density at horizon 1 allows us to perform drawings of future values of the process, by using the Sampling Importance Resampling (SIR) method [Gelfand, Smith (1992), Tanner (1993)] (see Section 6.1.4 for an illustration). To approximate the predictive density at horizon $h > 1$, for given Φ_1, Φ_2, \dots and g , we need S independent future paths of the process. Each path $s = 1, \dots, S$ is obtained by forecasting sequentially $Y_{T+1}^s|Y_T$, followed by $Y_{T+2}^s|Y_{T+1}^s, \dots, Y_{T+h}^s|Y_{T+h-1}^s$, from the predictive densities. This provides a drawing $Y_{T+1}^s, \dots, Y_{T+h}^s$ of a future path s . By replicating independently for $s = 1, \dots, S$, we get $Y_{T+h}^s, s = 1, \dots, S$ and can use their sample distribution as an estimator of the predictive distribution at horizon h .

4 Nonlinear Causal Innovations

In macroeconomics and finance, the use of the traditional causal VAR model commonly includes the IRF analysis, which is an important tool for the economists and financial policy makers. These tools are used for the so-called causal analysis. This terminology differs from the "causal-noncausal" terminology introduced by Rosenblatt in the context of time series, although they are related. More precisely, the "causal analysis" implies a) the possibility to make inference on the future from the past, i.e. to make forecasts and also b) the counterfactual analysis of the effects of current transitory shocks on the future. The standard linear causal IRF analysis cannot be applied to the mixed VAR(p) processes, because neither errors ε_t in model (2.1), nor state-specific linear innovations η_t in (3.8) are causal innovations independent of the lagged values of Y_t ⁶. Moreover the presence of noncausal roots in the mixed VAR model implies nonlinear causal dynamics, characterized by bubbles, for example. The nonlinearity has to be accounted for in the definition of causal innovations. In addition, these nonlinear causal innovations have to satisfy both the serial and cross-sectional independence conditions [Gourieroux, Jasiak (2005), Gourieroux, Monfort, Renne (2017)]. As mentioned earlier, the errors ε_t of mixed VAR models cannot be interpreted as innovations and then

⁶Some components of ε_t depend on the past values of Y_t . Then, it is difficult to interpret the shock on ε_t that implicitly changes a past that has already been realized [see Davis, Song (2020), Figures 1 and 7 for this practice].

used to define shocks and IRFs. We discuss below the filtering and identification of nonlinear causal innovations in the framework of mixed VAR models.

4.1 Definition of Nonlinear Innovations

The nonlinear causal innovations are defined below for any Markov process of order p , including any mixed VAR(p) model.

Definition 1: A nonlinear causal innovation of process (Y_t) is a process (v_t) of dimension m such that: i) the vectors v_t are serially i.i.d.; ii) the strictly stationary process (Y_t) can be written in a nonlinear autoregressive form:

$$Y_t = a(\underline{Y}_{t-1}, v_t). \quad (4.1)$$

iii) the future values \bar{v}_t of the innovation process are independent of the lagged values \underline{Y}_{t-1} of the observed process Y_t .

It is easy to see that conditions i) and ii) are equivalent to the Markov of order p property of (Y_t) with a continuous distribution, and can be applied to the mixed model (3.1) by Corollary 1 [see Appendix A.3 a)]. If function a is invertible with respect to v , then v_t is a nonlinear function of Y_t given its past and condition iii) is satisfied. Under conditions i) and ii) the autoregressive equation (4.1) can be applied recursively.

The nonlinear autoregressive model (4.1) is a nonlinear causal representation of the mixed VAR. The sequence of nonlinear causal innovations provide the basis of nonlinear impulse response functions [Potter (2000), Gouriéroux, Jasiak (2005)].

Let us consider a transitory shock δ at date T on v_T , and then apply recursively equation (4.1) to get the impulse response function for the future of the process:

$Y_T^\delta = a(Y_{T-1}^\delta, v_T + \delta)$, $Y_{T+1}^\delta = a(Y_T^\delta, Y_{T-1}, \dots, v_{T+1})$, and so on. The conditions i) and iii) in Definition 1 are crucial for the interpretation of shocks in terms of "causal analysis". Condition iii) means that v_T can be shocked at any time T without an effect on the realized past \underline{Y}_{T-1} . Condition i) means that this shock has no effect on the future values \bar{v}_{T+1} .

The nonlinear IRF defined above corresponds to a multivariate shock δ . The literature on "causal analysis" is also interested in univariate specific shocks. It is possible to define shocks on the component $v_{1,t}$ of v_t , if additionally the component $v_{1,t}$ and $(v_{2,t}, \dots, v_{n,t})$ are cross-sectionally independent.

4.2 Identification of Nonlinear Autoregression and Innovation

The nonlinear autoregression (4.1) depends on function a and on the distribution of the causal nonlinear innovation v_t . In the mixed VAR(p) model, these both depend on Φ_1, Φ_2, \dots and g , but do not satisfy a one-to-one relationship with them because the nonlinear function a depends on much more arguments than the density g .

This new nonparametric identification issue is examined in Appendix A.3 in a functional framework by using the properties of harmonic functions. In particular, we get the following Proposition:

Proposition 2:

In a mixed VAR(1) process, the dimension of under-identification in the functional space of nonlinear autoregressive models is finite and equal to $2m$.

This functional multiplicity is very large. Appendix A.3 shows that it is possible to restrict the analysis to nonlinear autoregressions with Gaussian innovations, such that the components $v_{1,t}, \dots, v_{n,t}$ are independent $N(0,1)$. However, this additional restriction is not sufficient to solve the identification issue. Indeed, there exist nonlinear transformations of v_t , with respect to which the multivariate $N(0, \text{Id})$ distribution remains invariant. As shown in Appendix A.3, they correspond to "local matrix rotations", i.e. rotations depending on the level v .

Corollary 3: Functional multiplicity

There exists a functional multiplicity of innovation processes (v_t) that are cross-sectionally independent standard normal variables.

Since the observed process (Y_t) and the state process (Z_t) satisfy a one-to-one relationship, for structural interpretations discussed below it is often preferable to consider nonlinear causal innovations to the state variables. The state variables satisfy also a nonlinear autoregressive scheme:

$$Z_t = \tilde{a}(Z_{t-1}, \tilde{v}_t), \quad (4.2)$$

where the \tilde{v}_t can be serially conditionally i.i.d. variables (possibly restricted to be standard Gaussian).

Therefore, the identification of nonlinear autoregressive representation of Gaussian nonlinear innovations and of nonlinear IRFs is a major issue in the mixed VAR models.

Example 1: The SVAR Model

For the structural causal VAR (SVAR) models, a similar identification issue has been recently solved [see, Online Appendix B]. More precisely, let us assume a causal SVAR model written as: $Y_t = \Phi_1 Y_{t-1} + \dots + \Phi_p Y_{t-p} + \varepsilon_t$, $\varepsilon_t = Du_t$, where the error term ε_t is a linear transform of independent sources u_t , with distributions g_1, \dots, g_n , respectively. Then, if at most one source is Gaussian, it is

possible to identify $\Phi_1, \dots, \Phi_p, D, g_1, \dots, g_n$ [see, Comon (1994) for ICA, Gouriou, Monfort, Renne (2017), (2020), Guay (2021), Bernoth et al. (2024) for the application to SVAR models]. Then the nonlinear autoregressive model is:

$$Y_t = \Phi_1 Y_{t-1} + \dots + \Phi_p Y_{t-p} + D \begin{pmatrix} G_1^{-1}[\Phi(v_{1,t})] \\ \vdots \\ G_1^{-1}[\Phi(v_{n,t})] \end{pmatrix},$$

where the components $v_{i,t}$ are independent standard normal variables, uniquely defined from $v_{i,t} = \Phi^{-1}[G_i(u_{i,t})]$, where G_i is the c.d.f. of g_i and Φ is the c.d.f. of the standard normal. Therefore the autoregressive function is the sum of a linear function of \underline{Y}_{t-1} and a nonlinear function of v_t . In macroeconomic applications, shocks with economic interpretations, such as the monetary shock, fiscal shock or productivity shock are usually applied to specific linear combinations $c'Y_t$ of the observed variables, which play the role equivalent to our state variables $z_t = c'Y_t$.

There exists a variety of methods to circumvent the functional identification issue.

i) In the applied literature, identifying restrictions of function a are often introduced by means of parametric assumptions on the joint distribution of errors ε_t . For example, one could choose this distribution among non-Gaussian elliptical parametric families based on t-Student distributions. However, such a partial identifying assumption is difficult to interpret due to the lack of structural interpretation of errors (ε_t).

ii) In special cases, a specific structural shock can appear. For example, the applications of mixed models indicate that the noncausal order is often equal to 1, i.e. $n_2 = 1$ [see e.g. Gouriou, Jasiak (2017), Hecq, Lieb, Telg (2016), and Section 6.3 of this paper]. This is likely due to the type of nonlinear dynamics generated by noncausal roots capturing the speculative bubbles and local trends. For example, in macroeconomic models, the noncausal component can be related to speculative bubbles in oil prices impacting jointly the price index, GDP and other macroeconomic variables. It is also common in financial applications based on nonlinear models with one factor capturing the nonlinear dynamics and interpreted as a systemic component. This explains the recent interest in common bubble [Gouriou, Zakoian (2017), Cubbada et al. (2023), Hall, Jasiak (2024)].

In the case $n_2 = 1$, with the interpretation of Z_2 as the systemic factor, it is insightful to examine the consequences of a shock to the latent noncausal component (Z_2), which determines the nonlinear dynamics of the model rather than to the observed variables. This can be done by applying nonlinear shock ordering to the pure causal and noncausal components (Z_t) and selecting Z_2 as the first variable to be shocked. To simplify the notation, we write v_t defined in equation (4.2) without the tilde. Then the nonlinear Gaussian causal innovation of Z_2 is uniquely defined as:

$$v_{2,t}(Z_t) = \Phi^{-1}[F_2(Z_{2,t}|\underline{Y}_{t-1})] = \Phi^{-1}[F_2(Z_{2,t}|Z_{t-1})], \quad (4.3)$$

where F_2 is the conditional cumulative distribution function (c.d.f) of $Z_{2,t}$. From equation (a.5) given in Appendix A.1, it follows that the conditional density of $Z_{2,t}$ given Z_{t-1} has a closed form given by:

$$l(z_{2,t}|z_{t-1}) = \frac{l_2(z_{2,t})}{l_2(z_{2,t-1})} |\det J_2| g_{\eta_2}(z_{2,t} - J_2 z_{2,t-1}), \quad (4.4)$$

where g_{η_2} is the marginal density of η_2 . The c.d.f. F_2 is the integral of $l(z_{2,t}|z_{t-1})$ over the set of admissible values of $z_{2,t}$.

Next, we can append it by searching for a possible Gaussian $(v_{2,t}, \dots, v_{n,t})$ associated with the causal state variables. This can be done recursively [see Appendix A.3]. For illustration, let us consider the case $n_1 = 1$ and define:

$$v_{1,t}(Z) = \Phi^{-1}[F_{1|2}(Z_{1,t}|Z_{2,t}, Z_{t-1})], \quad (4.5)$$

where $F_{1|2}$ is the conditional cumulative distribution function of $Z_{1,t}$ given $Z_{2,t}, Z_{t-1}$. From equation (a.5) in Appendix A.1, we get the closed-form expression of the conditional density:

$$l(z_{1,t}|z_{2,t}, z_{t-1}) = l(z_t|z_{t-1})/l(z_{2,t}|z_{t-1}) = \frac{g_{\eta_1}(z_{1,t} - J_1 z_{1,t-1}, z_{2,t} - J_2 z_{2,t-1})}{g_{\eta_2}(z_{2,t} - J_2 z_{2,t-1})}. \quad (4.6)$$

The c.d.f. $F_{1|2}$ is the integral of $l(z_{1,t}|z_{2,t}, z_{t-1})$ over the set of admissible values of $z_{1,t}$.

When the variable Z_2 defines the selected "ordering" it is easy to check that $v_{1,t}(Z)$ differs in general from the causal innovation $\eta_{1,t}$ to the latent causal component $Z_{1,t}$. By applying the ordering, we see from (4.3)-(4.5) that the autoregressive model can be written under a recursive form. Moreover, we deduce from (4.4):

Corollary 4:

The noncausal state variable $(Z_{2,t})$ is a Markov process of order 1 with respect to the filtrations associated with (Y_t) , (Z_t) and $(Z_{2,t})$.

By construction, the structural noncausal shock $v_{2,t}(Z_t)$ is defined in a unique way (since $n_2 = 1$) and is a Gaussian white noise ⁷. It is also independent of the multivariate shock $v_{1,t}(Z_t)$. Then, we can construct nonlinear IRFs for Y based on the effect of a change δ_2 in $v_{2,t}$, with $v_{1,t}$ held constant. It is called the Common Bubble Shock (CBS) henceforth. In the general case $n_2 = 1, n_1 \geq 1$, the associated multivariate impulse responses of $Z_{2,t}$ are identifiable, i.e. independent of other components $(v_{1,t}, v_{3,t}, \dots, v_{n,t})$.

⁷See Gourieroux, Jasiak (2005) for the uniqueness of nonlinear Gaussian innovation in a univariate model.

5 Statistical Inference

The parameters of a mixed VAR model need to be estimated before the forecasts and nonlinear causal innovations are computed. The first part of this Section reviews the estimation methods that exist in the literature and describes the new prediction/filtering algorithm for the estimated nonlinear causal innovations. Next, we introduce a post-estimation inference method for assessing the prediction interval uncertainty due to the preliminary estimation step.

5.1 Estimation and Filtering

The mixed VAR model can be estimated by the maximum likelihood method based on an assumed parametric distribution of ε_t [see Breidt et al. (1991), Lanne, Saikkonen (2010), (2013), Davis, Song (2020), Bec et al. (2020)]. This approach yields consistent estimators provided that the parametric distributional assumption is well specified.

Alternatively, the mixed VAR model can be consistently estimated without any parametric assumptions on the distribution of the errors ⁸ by using the (Generalized) Covariance (GCov) estimator [Gourieroux, Jasiak (2022)]. The GCov estimator is consistent, asymptotically normally distributed and semi-parametrically efficient. As an alternative, minimum distance estimators based on the cumulant spectral density of order 3 and 4 have been proposed in Velasco, Lobato (2019) and Velasco (2022) ⁹.

The prediction and filtering methods introduced in Sections 3,4 for given Φ_1, \dots, Φ_p and g can be applied in a parametric or semi-parametric framework by replacing the unknown parameters by their consistent estimates. In the semi-parametric framework, it can be applied along the following lines:

step 1. Apply the GCov estimator based on zero auto-covariance conditions of nonlinear error functions to obtain the estimators of matrices of autoregressive coefficients $\hat{\Phi}_1, \dots, \hat{\Phi}_p$.

step 2. Use the $\hat{\Phi}_i, i = 1, \dots, p$, estimates to compute the roots of the lag-polynomial and more generally an estimated Jordan representation: $\hat{A}, \hat{J}_1, \hat{J}_2$.

step 3. Compute the approximated model errors using the estimates obtained in Step 1: $\hat{\varepsilon}_t = Y_t - \hat{\Phi}_1 Y_{t-1} - \dots - \hat{\Phi}_p Y_{t-p}$.

step 4. Compute $\hat{Z}_t = \hat{A}^{-1} \begin{pmatrix} Y_t \\ \tilde{Y}_{t-1} \end{pmatrix}$, $\hat{\eta}_t = \hat{A}^{-1} \begin{pmatrix} \hat{\varepsilon}_t \\ 0 \end{pmatrix}$.

step 5. The following densities can be estimated by kernel estimators applied to the approximated series:

⁸Except for the non-Gaussianity assumption.

⁹See also Starck (2023) for a two-step continuum method of moments. The method of moment estimators provide consistent estimators only in applications to the VAR models satisfying the additional cross-sectional independence condition [see, Guay (2021)].

- the density g of ε_t can be estimated from $\hat{\varepsilon}_t$, $t = 1, \dots, T$;

- the density l_2 of $Z_{2,t}$ can be estimated from $\hat{Z}_{2,t}$, $t = 1, \dots, T$;

step 6. The predictive density can be estimated from the formula of Proposition 2 by replacing l_2 by \hat{l}_2 , A^2 by \hat{A}^2 , and also J_2 by \hat{J}_2 , g by \hat{g} , and Φ_1, \dots, Φ_p by $\hat{\Phi}_1, \dots, \hat{\Phi}_p$. The mode (median) of the predictive density provides the point forecasts and the quantiles of the predictive density can be used to obtain estimated prediction intervals at horizon 1.

When there is a single non-causal state variable this can be completed by:

step 7. The approximations of nonlinear causal innovations $\hat{v}_{2,t}(Z)$ can be computed from the estimated distributions as $\hat{v}_{2,t}(Z) = \Phi^{-1}(\hat{F}_{2,T}(\hat{Z}_{2,t}|\hat{Z}_{t-1}))$ by applying the formula of predictive density (4.3) with l_2 replaced by \hat{l}_2 and g_{η_2} replaced by \hat{g}_{η_2} , i.e. the empirical density of $\hat{\eta}_{2,t}$, $t = 1, \dots, T$.

step 8. Next, they can be appended by the approximated nonlinear causal innovations independent of $\hat{v}_{2,t}(Z)$ such as

$$\hat{v}_{1,t} = \Phi^{-1}(\hat{F}_{1|2,T}(\hat{Z}_{1,t}|\hat{Z}_{2,t}, \hat{Z}_{t-1})), \text{ for } n_1 = 1.$$

These causal innovations can be computed from the predictive density formula (4.5) with g_{η_2} and g_{η_1} replaced by their empirical counterparts.

5.2 Uncertainty of the Estimated Prediction Set

The estimated model parameters and residuals $\hat{\varepsilon}_t$ can be used to build oos forecast intervals conditional on given values of the last observations in the sample, called the conditional prediction interval. The estimation errors associated with the scalar and functional parameters have an effect on the uncertainty of the conditional prediction interval. We provide below a detailed framework in which various notions of prediction sets can be distinguished.

i) True Prediction Interval

For ease of exposition, let us consider the VAR(1) model, forecast horizon $h = 1$ and future value of the first component series $Y_{1,T+1}$ to be forecast at date T out of sample (oos) given $Y_T = (y_{1,T}, y_{2,T})' \equiv y$, where $(Y_{2,t})$ contains the remaining components of the series. Then, the true prediction interval at level $1 - \alpha_1$ for $Y_{1,T+1}$ is:

$$PI(y, \alpha_1) = [Q_l(y, \alpha_1; P_0), Q_u(y, \alpha_1; P_0)], \quad (5.1)$$

where P_0 is the true distribution function of process (Y_t) and $Q(y, \alpha, P_0)$ denotes the α -quantile of $Y_{1,T+1}$ conditional on $Y_T = y$ and derived from the joint multivariate predictive density $l(y|\underline{Y}_T)$ (see Proposition 1 for the closed-form expression of the predictive density). Let Q_l and Q_u denote the true $\alpha_1/2$ and $1 - \alpha_1/2$ conditional quantiles, respectively. Recall that under the semi-parametric approach, the true distribution P_0 is characterized by Φ_0 and g_0 . By using the expression of the

prediction interval in a Gaussian framework, the asymptotically valid prediction interval for $Y_{1,T+1}$ can be equivalently written as:

$$PI(y, \alpha_1) = [m(y, \alpha_1; P_0) \pm \Phi^{-1}(\alpha_1/2) \sigma(y, \alpha_1; P_0)], \quad (5.2)$$

with ¹⁰

$$m(y, \alpha_1; P_0) = 0.5[Q_l(y, \alpha_1; P_0) + Q_u(y, \alpha_1; P_0)], \quad (5.3)$$

$$\text{and } \sigma(y, \alpha_1; P_0) = -[1/(2\Phi^{-1}(\alpha_1/2))][Q_u(y, \alpha_1; P_0) - Q_l(y, \alpha_1; P_0)]. \quad (5.4)$$

This normalized representation of the prediction interval resembling the traditional Gaussian approach can be used even if the conditional density function of (Y_t) is not Gaussian. In particular, the functions $y \rightarrow m(y, \alpha_1; P_0)$, $y \rightarrow \sigma(y, \alpha_1; P_0)$ are nonlinear, in general.

ii) Estimated Prediction Interval

In our framework, the unknown marginal predictive density function P_0 can be consistently estimated from its expression (3.12) as \hat{P} , given the estimated matrix of autoregressive parameters $\hat{\Phi}$ and the residuals $\hat{\varepsilon}_t$ obtained from the semi-parametric GCov estimator that provides the nonparametric estimator \hat{g} . Then, we can compute an estimated prediction interval of $Y_{1,T+1}$:

$$\widehat{PI}(y, \alpha_1) = [m(y, \alpha_1; \hat{P}) \pm \Phi^{-1}(\alpha_1/2) \sigma(y, \alpha_1; \hat{P})] = [Q_l(y, \alpha_1; \hat{P}), Q_u(y, \alpha_1; \hat{P})]. \quad (5.5)$$

where $Q_l(y, \alpha_1; \hat{P})$ and $Q_u(y, \alpha_1; \hat{P})$ are the $\alpha_1/2$ and $1 - \alpha_1/2$ conditional quantiles of the estimated predictive density.

This estimated prediction interval (5.5) is consistent of the true prediction interval (5.2) when the number of observations tends to infinity. We need to distinguish:

a) the true prediction interval $PI(y, \alpha_1)$ of $Y_{1,T+1}$ satisfying $P_0[Y_{1,T+1} \in PI(y, \alpha_1) | Y_T = y] = 1 - \alpha_1, \forall y$.

By construction, the true prediction interval has the correct conditional coverage probability of $1 - \alpha_1$. It depends on the unknown true distribution, or equivalently on Φ_0, g_0 .

b) The estimated prediction interval $\widehat{PI}(y, \alpha_1)$ that does not satisfy the conditional coverage condition in finite sample: $P_0[Y_{1,T+1} \in \widehat{PI}(y, \alpha_1) | Y_T = y] \neq 1 - \alpha_1, \forall y$.

due to the estimation errors.

iii) Bootstrap Adjusted Prediction Interval

Since this estimated prediction interval is random, its asymptotic distribution can be approximated by bootstrap, which is applied by replicating the trajectory of the process by backcasting.

¹⁰Note that $\Phi^{-1}(\alpha_1/2)$ is negative.

More precisely, given $\hat{\Phi}$, \hat{g} considered fixed and the residuals, we can generate by backcasting the artificial paths Y_t^s , $t = 1, \dots, T$ with the same terminal condition $Y_T^s = Y_T = y$ for all the bootstrapped samples (see, Corollary 2 for the closed-form expression of the backward predictive distribution).

The backcasting can be performed as the following sequence of one-step backcasts:

step 1: Starting from Y_T , we backcast Y_{T-1}^s , conditional on Y_T , next we backcast Y_{T-2}^s conditional on Y_{T-1}^s , and so on.

Step 2: By replicating the backcasted path S times, we end up generating S bootstrapped series $Y_t^s, t = 1, \dots, T$ of length T equal to the length of the initial series and with the same terminal value Y_T .

step 3: From each replicated path ($Y_t^s, t = 1, \dots, T$), we estimate the model parameters Φ^s and \hat{g}^s , $s = 1, \dots, S$. That allows us for computing at Y_T the predictive density estimator \hat{P}^s , $s = 1, \dots, S$ of Y_{T+1} given Y_T and S new prediction intervals of $Y_{1,T+1}$ from each of the replicated paths.

step 4: The bootstrapped prediction interval obtained from a replicated path is:

$$\widehat{PI}^s(y, \alpha_1) = [m(y, \alpha_1; \hat{P}^s) \pm \Phi^{-1}(\alpha_1/2)\sigma(y, \alpha_1; \hat{P}^s)], \quad (5.6)$$

where \hat{P}^s is the semi-parametric estimate of P_0 from the artificial path ($Y_t^s, t = 1, \dots, T$). Given $\hat{P}^s, s = 1, \dots, S$ of Y_{T+1} this bootstrap PI of $Y_{1,T+1}$ given Y_T can be replicated independently $s = 1, \dots, S$ times.

The components of the prediction interval (5.6) are denoted by:

$$\hat{m}^s(y, \alpha_1) = m(y, \alpha_1; \hat{P}^s), \quad \hat{\sigma}^s(y, \alpha_1) = \sigma(y, \alpha_1; \hat{P}^s), \quad s = 1, \dots, S. \quad (5.7)$$

step 5: For large S , the joint sample distribution of $[\hat{m}^s(y, \alpha_1), \hat{\sigma}^s(y, \alpha_1)]$ provides an approximation of the distribution of $[m(y, \hat{P}), \sigma(y, \hat{P})]$, when T is finite and sufficiently large.

5.3 Confidence Interval of the Prediction Interval

The estimated prediction interval $\widehat{PI}(y, \alpha_1)$ is a pointwise estimator of interval $PI(y, \alpha_1)$ and as any estimator, is random itself. This randomness is difficult to assess since $\widehat{PI}(y, \alpha_1)$ is a random set (interval). Let us now extend the method of pointwise estimation to build confidence sets for $PI(y, \alpha_1)$. Since there does not exist a total ordering on intervals, we first constrain the confidence set to be of the form:

$$\widehat{PI}(y, \alpha_1, q) = [m(y, \alpha_1; \hat{P}) \pm q\sigma(y, \alpha_1; \hat{P})]. \quad (5.8)$$

and search for an estimator of q providing the correct asymptotic coverage. This confidence set has the following coverage probability of the true prediction interval:

$$\begin{aligned}
\Pi_0(y, \alpha_1; q) &= P_0[\widehat{PI}(y, \alpha_1, q) \supset PI(y, \alpha_1) | Y_T = y] \\
&= P_0[m(y, \alpha_1; \hat{P}) - q \sigma(y, \alpha_1; \hat{P}) < m(y, \alpha_1; P_0) + \Phi^{-1}(\alpha_1/2) \sigma(y, \alpha_1; P_0), \\
&\quad m(y, \alpha_1; \hat{P}) + q \sigma(y, \alpha_1; \hat{P}) > m(y, \alpha_1; P_0) - \Phi^{-1}(\alpha_1/2) \sigma(y, \alpha_1; P_0) | Y_T = y], \quad (5.9)
\end{aligned}$$

because $\Phi^{-1}(\alpha_1/2) < 0$. For $\alpha_2 \in (0, 1)$, possibly different from α_1 , there exists a value $q_0(y, \alpha_1; \alpha_2)$ such that:

$$\Pi_0[y, \alpha_1; q_0(y, \alpha_1; \alpha_2)] = 1 - \alpha_2. \quad (5.10)$$

Asymptotically, we get the $1 - \alpha_2$ coverage probability of the true conditional prediction interval, although the true predictive density P_0 and the true distribution of \hat{P} remain unknown.

Therefore, equations (5.9) and (5.10) can be replaced by their bootstrapped counterparts obtained from S replicated paths of the series. More precisely, the bootstrapped conditional coverage probability is defined as:

$$\hat{\Pi}^s(y, \alpha_1, q) = \frac{1}{S} \sum_{s=1}^S \delta^s,$$

where

$$\delta^s = \begin{cases} 1, & \text{if } \hat{m}^s(y, \alpha_1) - q \hat{\sigma}^s(y, \alpha_1) < \hat{m}(y, \alpha_1) + \Phi^{-1}(\alpha_1/2) \hat{\sigma}(y, \alpha_1), \\ & \text{and } \hat{m}^s(y, \alpha_1) + q \hat{\sigma}^s(y, \alpha_1) > \hat{m}(y, \alpha_1) - \Phi^{-1}(\alpha_1/2) \hat{\sigma}(y, \alpha_1), \\ 0, & \text{otherwise.} \end{cases}$$

Then, we consider a solution $\hat{q}(y, \alpha_1, \alpha_2)$ of:

$$\hat{\Pi}^s[y, \alpha_1, \hat{q}(y, \alpha_1, \alpha_2)] = 1 - \alpha_2. \quad (5.11)$$

ensuring the $1 - \alpha_2$ coverage probability. The bootstrap confidence set of the prediction interval is:

$$\widehat{CSPI}(y, \alpha_1, \alpha_2) = \left\{ m(y, \alpha_1, \hat{P}) \pm \hat{q}(y, \alpha_1, \alpha_2) \sigma(y, \alpha_1, \hat{P}) \right\}. \quad (5.12)$$

This bootstrap confidence set is such that:

$$\lim_{T \rightarrow \infty} \lim_{S \rightarrow \infty} P_0[\widehat{CSPI}(y, \alpha_1, \alpha_2) \supset PI(y, \alpha_1) | Y_T = y] = 1 - \alpha_2, \quad \forall P_0. \quad (5.13)$$

Hence, the length of the estimated $\widehat{PI}(y, \alpha_1)$ is enlarged by a factor $\hat{q}(y, \alpha_1, \alpha_2)/|\Phi^{-1}(\alpha_1/2)|$, that depends on the observed value y , in general. In practice, we can choose $\alpha_1 = \alpha_2 = 0.05$ corresponding to the standard levels for prediction and confidence intervals, respectively. One could also choose α_1 different from α_2 , including $\alpha_1 = 1.0$, which would correspond to the confidence set of point prediction equal to the median of the predictive density.

The analysis of a confidence set of the prediction set is related to research on a confidence set of the identified set in models under partial identification. The partial identification literature

considers a parametric model with a parameter γ , say, that is partly identifiable¹¹. The objective is to determine either the confidence set under the classical approach, or the credible set under the Bayesian approach. In our framework, we have two types of "parameters", P and $Y_{1,T+1}$, say. The second one is not identifiable, although its conditional distribution is estimated, and plays the role of a conditional prior.

6 Illustration

We illustrate the nonlinear forecasts from the mixed VAR(1) model. The first part of this Section presents a simulation study that examines the out of sample forecasts from the model. Next, the semi-parametric GCov estimation, nonlinear innovations and CBS are illustrated in applications to the joint analysis of a bivariate series of Bitcoin/USD and Ethereum/USD exchange rates.

6.1 Simulation Study

6.1.1 The Artificial Data Set

We consider a simulated bivariate mixed VAR(1) process with the following matrix Φ of autoregressive coefficients and matrix A :

$$\Phi = \begin{pmatrix} 0.7 & -1.3 \\ 0 & 2 \end{pmatrix}, \quad A = \begin{pmatrix} 1 & -1 \\ 0 & 1 \end{pmatrix}.$$

where matrix Φ has eigenvalues 0.7 and 2, located inside and outside the unit circle, respectively¹². The errors follow a bivariate noise with independent components both t-student distributed with $\nu = 4$ degrees of freedom, mean zero and variance equal to $\nu/(\nu - 2) = 2$.

The simulated paths of the series of length 600 are displayed in Figure 1. The solid (black) line represents process Y_{1t} and the dashed (red) line represents process Y_{2t} .

The sequence of spikes in the noncausal component $Y_{2t} = Z_{2t}$ impacts the component Y_{1t} through the recursive form of matrix Φ .

6.1.2 Estimated Predictive Density, Point and Interval Forecasts

Let us now consider forecasts based on the estimated model parameters. The Generalized Covariance (GCov) estimate of matrix Φ is obtained by minimizing the portmanteau statistic computed from the auto- and cross-correlations up to and including lag $H = 10$ of the errors $\varepsilon_t = Y_t - \Phi_1 Y_{t-1}$

¹¹See Imbens, Manski (2004) for confidence intervals of identified intervals in the framework of partial identification and confidence intervals that asymptotically cover the true interval with a probability larger or equal to $1 - \alpha_2$.

¹²The finite sample properties of the GCov estimator are illustrated in Gouriéroux, Jasiak (2017).

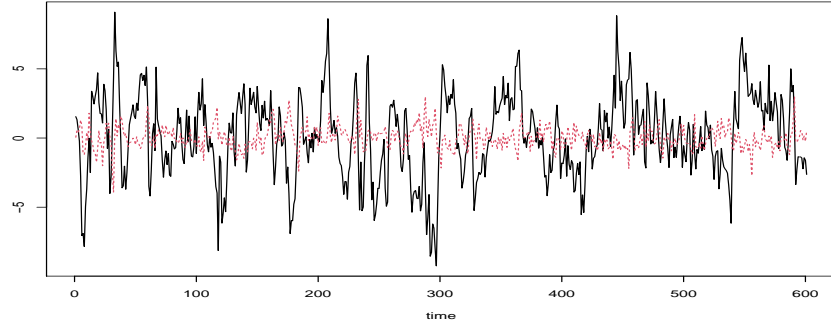


Figure 1: Bivariate Mixed VAR(1) Process: Y_1 : solid line, Y_2 : dashed line

and their squared values [see Gouriou, Jasiak (2022)]. The following estimated autoregressive matrix is obtained:

$$\hat{\Phi} = \begin{pmatrix} 0.724 & -1.452 \\ -0.030 & 1.993 \end{pmatrix},$$

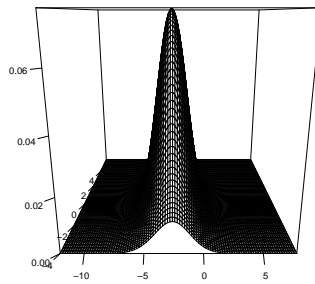
with eigenvalues $\hat{\lambda}_1 = 0.690$, $\hat{\lambda}_2 = 2.027$ close to the true values $\lambda_1 = J_1 = 0.7$ and $\lambda_2 = J_2 = 2.0$. The standard errors of $\hat{\Phi}$ obtained by bootstrap are 0.023, 0.308, for the elements of the first row, and 0.009, 0.120 for the elements of the second row.

After estimating Φ , the GCov estimated errors $\hat{\varepsilon}_t = Y_t - \hat{\Phi}Y_{t-1}$ are computed and used for forecasting. Matrices A and A^{-1} are identified from the Jordan representation of matrix Φ , up to scale factors. The estimated matrix \hat{A}^{-1} computed from the normalized Jordan decomposition of $\hat{\Phi}$ is:

$\hat{A}^{-1} = \begin{pmatrix} 0.022 & 0.025 \\ -0.022 & 0.974 \end{pmatrix}$. It corresponds to matrix $A^{-1} = \begin{pmatrix} 1 & 1 \\ 0 & 1 \end{pmatrix}$ up to scale factors of about 0.02 and 0.97 for each column.

Let us now consider the oos nonlinear forecast one step ahead performed at date $T = 590$. At time $T=590$, the process takes values -3.367 and -0.239. The true values of Y_1 and Y_2 at $T+1=591$ are -2.260 and -0.331, respectively. The nonlinear forecasts are summarized by the predictive density that can be used to compute the pointwise predictions of $Y_{1,T+1}$ and $Y_{2,T+1}$. The predictive bivariate density is estimated and shown in Figure 2 along with the estimated predictive marginal densities of $Y_{1,T+1}$ and $Y_{2,T+1}$, respectively. The predictive density is estimated from formula (3.12) one-step ahead oos by using a kernel estimator over a grid of 100 values below and above Y_1 and Y_2 , with Gaussian kernels and bandwidths $h_2 = 1$ and $h_{11} = s.d.(\varepsilon_1)$, $h_{12} = s.d.(\varepsilon_2)$ (see On-Line Appendix C for kernel density estimators).

The estimated point forecasts are obtained from the mode of the predictive density. The forecast of $Y_{1,591}$ based on the GCov estimated parameters is -2.80 and the point forecast of $Y_{2,591}$ is -0.30. The estimated prediction intervals at level 0.80 determined from the predictive density are as follows: The estimated prediction interval for $Y_{1,591}$ at level 0.80 is [-4.80, -0.80] and the prediction interval



(a) Estimated Joint Predictive Density

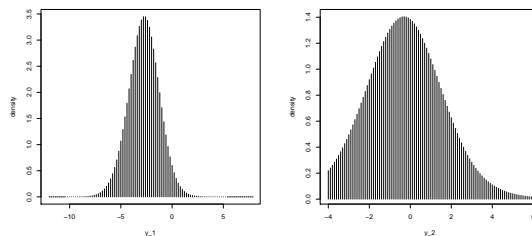
(b) $Y_{1,T+1}$ (c) $Y_{2,T+1}$

Figure 2: Estimated Predictive Joint and Marginal Densities

for $Y_{2,591}$ is $[-2.60, 2.10]$. The rationale for choosing level 80% is to ensure a sufficiently large number of observations in the tails for computing the quantiles of the predictive density. Both prediction intervals contain the true future values of the process.

Next, we compute oos one-step ahead forecasts based on the sub-sample of 500 observations on Y_t . Figure 3 displays 100 one-step ahead oos forecasts along the trajectory.

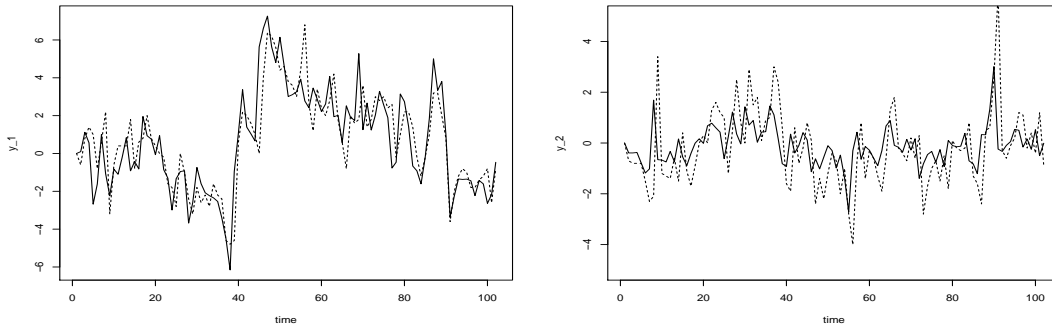
6.1.3 Unconditional Coverage of the Estimated Prediction Interval

Let us now consider a bivariate VAR(1) with the autoregressive matrix:

$$\Phi = \begin{pmatrix} 0.9 & -0.3 \\ 0.0 & 1.2 \end{pmatrix},$$

and eigenvalues $\lambda_1 = 0.9$, $\lambda_2 = 1.2$, which are closer to the unit circle. The errors ε_t have an identity variance-covariance matrices and t-student distributions with 3, 6 and 9 degrees of freedom.

The simulated bivariate series are of length 100, 500 and 1000 and the DGP is replicated 500 times. The last observation from each simulated path is set aside. It is forecast and used for forecast coverage assessment. The autoregressive parameters $\hat{\Phi}$ are estimated by the GCov estimator from the errors $\varepsilon_t = Y_t - \Phi_1 Y_{t-1}$, their second, third and fourth powers, and their lags up to $H = 10$. The objective function maximizing algorithm is each time initiated at the starting values 0.1, 0.1, 0.5, 0.5. The oos predictive density given in equation (3.12) of $y(1000)$ is evaluated, given the parameter estimates, over a grid of 100 possible future values for each of the components series.



(a) Estimated 1-step-ahead Forecasts of $Y_{1,t}$ (b) Estimated 1-step-ahead Forecasts of $Y_{2,t}$

Figure 3: Estimation-Based oos One-Step Ahead Forecasts true:solid line, forecast:dashed line

We use Gaussian kernels and bandwidths $h_2 = s.d.(Y_{2,t})$, $h_{11} = s.d.(\varepsilon_1)$ and $h_{12} = s.d.(\varepsilon_2)$ (see On-Line Appendix C for kernel density estimators). The mode of the predictive density estimated from formula (3.12) with Gaussian kernels provides the point forecast. The oos prediction intervals at horizon 1 are obtained from the marginal 10th and 90th percentiles of the bivariate predictive density. As before, the rationale for choosing level 80% is to ensure a sufficiently large number of observations in the tails for computing the quantiles of predictive densities.

The unconditional coverage of the estimated prediction interval is reported in Table 1 below for the sample sizes $T=500$ and $T=1000$ and t-student error ε_t distributions with 3, 6 and 9 degrees of freedom.

Table 1: Coverage of GCov Estimated Prediction Interval at 80%

	T=100			T=500			T=1000		
VAR(1) with eigenvalues 0.9, 1.2									
component	t(3)	t(6)	t(9)	t(3)	t(6)	t(9)	t(3)	t(6)	t(9)
$y_1(T+1)$	80.2	82.8	87.4	82.2	86.0	84.2	84.6	84.4	88.6
$y_2(T+1)$	90.4	89.4	90.8	90.6	91.6	92.40	91.4	91.0	92.8

We observe that the coverage is either greater or close to the theoretical size of the prediction interval for all sample sizes. Then, the bootstrap adjustment could be applied.

6.1.4 Estimated Prediction Set Uncertainty

This Section illustrates the uncertainty on the conditional prediction interval described in Section 5.2. We consider the simulated trajectory of length $T=200$ of the bivariate VAR(1) process with autoregressive matrix, illustrated in Table 1 with eigenvalues $\lambda_1 = 0.9$, $\lambda_2 = 1.2$ and $t(6)$ distributed errors with an identity variance-covariance matrix.

We are interested in the conditional prediction interval out-of-sample of the first component $Y_{1,T+1} = Y_{1,200}$ given the past and current values of the two series.

The mixed VAR(1) model is estimated by the GCov estimator from the observations $t = 1, \dots, 199$ with four power transforms of model errors and lag $H = 10$, providing the following estimates of the autoregressive parameters: 0.8931, -0.2146, 0.0180, 1.2797, and the following estimates of eigenvalues: 0.903 and 1.269.

The estimated predictive density of Y_{200} conditional on Y_{199} is computed from formula (3.12) by using kernel smoothed density estimators. More specifically, we employ Gaussian kernels and bandwidths $h_2 = s.d.(Y_2), h_{11} = s.d.(\varepsilon_1), h_{12} = s.d.(\varepsilon_2)$ (see On-Line Appendix C for kernel density estimators). For $\alpha_1 = 0.2$ and $\Phi^{-1}(\alpha_1/2) = -1.28$, the estimated prediction interval of $Y_{1,T+1} = Y_{1,200}$ is $\widehat{PI}(y, \alpha_1) = [-6.954, 0.360]$. It contains the true value of $Y_{1,200} = -0.696$.

In the next step, we replicate the initial paths $S = 50$ times by backcasting from the bivariate terminal condition $Y_{199} = [-1.188, 0.473]$. We use the backcasting formula given in Corollary 2, evaluated from estimated model parameters and kernel density estimators. We employ Gaussian kernels and bandwidths $h_1 = s.d.(Y_{1,t}), h_{11} = s.d.(\varepsilon_1)$ and $h_{12} = s.d.(\varepsilon_2)$.

The randomness of the backcasted paths is generated as follows: i) We first draw 100 values as if the components $Y_{1,T-1}, Y_{2,T-1}$ were independent conditional on Y_T . This is done by inverting the estimated conditional c.d.f.s of $Y_{1,T-1}$ and $Y_{2,T-1}$ given Y_T . This provides the sampling with the importance (misspecified) density; ii) Next, we re-sample in the set of values obtained in step i) above, with the weights proportional to the ratio of the joint backward predictive density divided by the product of the two marginal backward predictive densities. This procedure adjusts for the omitted cross-sectional dependence in step i).

The parameter Φ and functional parameter g are re-estimated from each replicated path, and then the values of $\hat{m}^s, \hat{\sigma}^s$ are computed from the quantiles of 50 predictive densities of Y_{T+1} conditional on Y_T . They are next used to compute the bootstrap confidence interval at level $\alpha_2 = 0.1$ of the prediction interval $\widehat{CSPI}(y, \alpha_1, \alpha_2) = [-11.839, 5.246]$, with the solution $\hat{q}(y, \alpha_1, \alpha_2) = 2.99$. The confidence interval \widehat{CSPI} of the prediction interval is much larger than the interval \widehat{PI} . This result illustrates the importance of taking into account the estimation risk on Φ, g when providing a prediction interval, especially that the estimator of the functional parameter g converges at a lower speed than the parameter estimator. The effect of estimation risk is twofold: i) the length of the interval has almost doubled, ii) the interval became less symmetric with respect to 0.

6.2 Application to Cryptocurrency Prices

Cryptocurrency rates often display speculative bubbles and can be modelled as mixed VAR models [see e.g. Gouriéroux, Hencic (2015) for an early paper on cryptocurrency dynamics and Hall, Jasiak

(2024)]. Since 2021, the cryptocurrency market has evolved towards becoming better organized and regulated. First, various cryptocurrency indexes have appeared, including the S&P Bitcoin Index, S&P Ethereum Index and the S&P Cryptocurrency MegaCap Index for tracking separately and jointly the performance of the cryptocurrencies with the highest capitalization, Bitcoin and Ethereum. The current market capitalizations of Bitcoin (BTC) and Ethereum (ETH) are of about 938.3 and 363.41 billion USD, respectively. More recently, several Exchange Traded Funds (ETF) for cryptocurrency became available. On January 10, 2024, the SEC (Securities and Exchange Commission) approved the listing and trading of crypto ETF shares on registered securities exchanges in the US, indirectly opening this market to retail investors¹³. This development marks the beginning of a new episode in the cryptocurrency markets and motivates our empirical study of Bitcoin and Ethereum.

Estimation

Let us consider the bivariate series of Bitcoin and Ethereum prices in US Dollars. The bivariate series of 257 daily adjusted closing BTC/USD and ETH/USD exchange rates recorded between July 21, 2021 and April, 04, 2022¹⁴ are displayed in Figure 4.

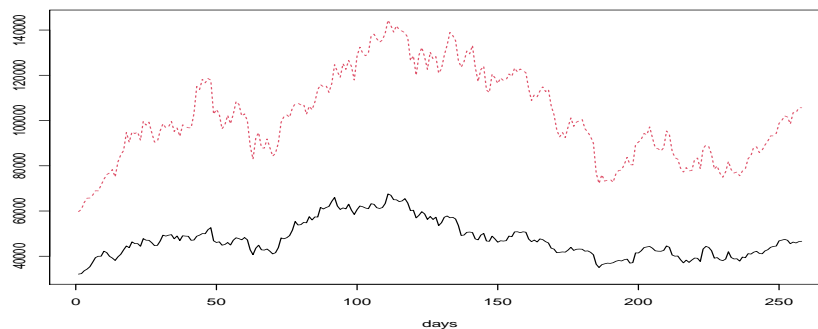


Figure 4: BTC/USD and ETH/USD Daily Closing Rates, July 21, 2021 to April 04, 2022
BTC/USD: solid black line, ETH/USD (times 30): dashed red line

We observe that both series display comovements over time and their dynamics are characterized by spikes and local trends/bubbles.

The bivariate VAR model is estimated from the data rescaled and adjusted by a polynomial function of time of order 2 for the hump-shaped pattern in the middle of the sampling period. This pre-filtering by a deterministic function is used instead of a moving average filter that could create spurious noncausal effects. The estimation is performed without imposing any distributional assumptions on the errors. We use the semi-parametrically efficient GCov estimator with nonlinear transformations including powers two, three and four of the errors summed up to lag 10. The

¹³The OSC (Ontario Securities Commission) approved a Bitcoin ETF in February 2021.

¹⁴Data Source: Yahoo Finance Canada <https://ca.finance.yahoo.com/>

estimated matrix $\hat{\Phi}$ is:

$$\hat{\Phi} = \begin{pmatrix} -0.0901 & 1.1998 \\ 0.4183 & 0.7724 \end{pmatrix},$$

with eigenvalues -0.488 and 1.171. Hence, there is a single noncausal component that captures the common bubbles and spikes. The standard errors of $\hat{\Phi}_{1,1}$ and $\hat{\Phi}_{1,2}$ are 0.014 and 0.013. For $\hat{\Phi}_{2,1}$ and $\hat{\Phi}_{2,2}$ the standard errors take values 0.022 and 0.019, respectively. To check the assumption of serial independence of errors ε_t , Figures 5 and 6 provide the autocorrelations of the approximated errors and their squares. They indicate that the error is close to a bivariate white noise and the model provides a satisfactory fit.

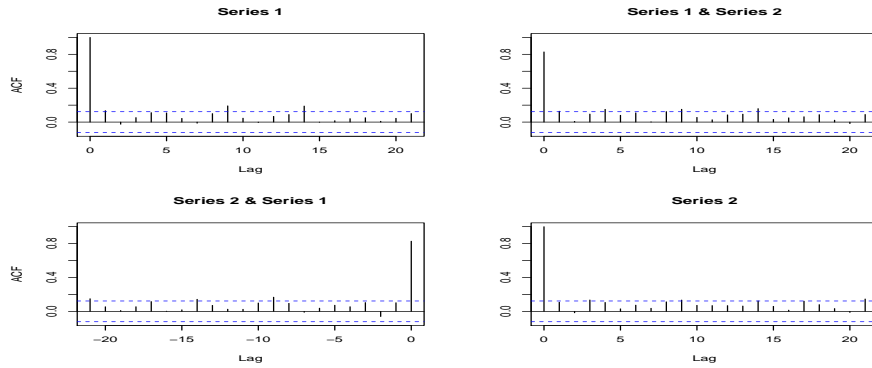


Figure 5: ACF of $\hat{\varepsilon}_t$

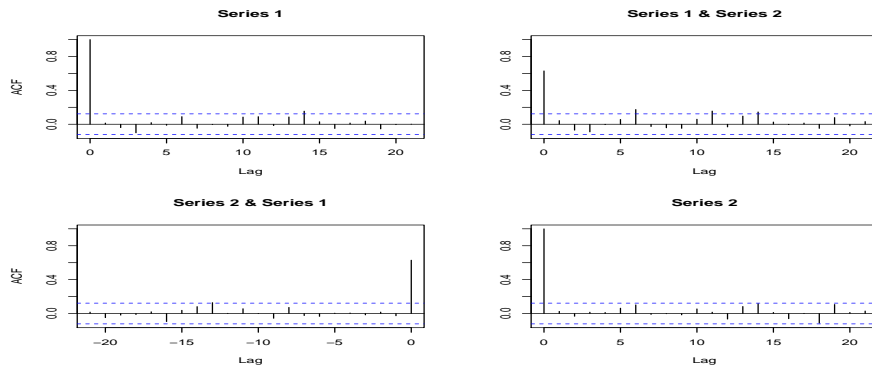


Figure 6: ACF of Squared $\hat{\varepsilon}_t$

The Jordan decomposition of matrix $\hat{\Phi}$ is: $\hat{\Phi} = \hat{A}\hat{J}\hat{A}^{-1}$, with

$$\hat{A} = \begin{pmatrix} -3.013 & 0.951 \\ 1 & 1 \end{pmatrix}, \hat{J} = \begin{pmatrix} -0.488 & 0 \\ 0 & 1.171 \end{pmatrix}, \hat{A}^{-1} = \begin{pmatrix} -0.252 & 0.240 \\ 0.252 & 0.759 \end{pmatrix}.$$

Forecasting

We illustrate the forward prediction method by forecasting the adjusted closing BTC/USD and ETH/USD exchange rates on April 4, 2022 ¹⁵ equal to 46622.67 and 3521.24, respectively. The

¹⁵This last observation is excluded from the estimation.

point forecast of demeaned and rescaled $y_{1,T+1}$ is -740.00, and the forecast of demeaned $y_{2,T+1}$ is 105.00. The forecast interval of y_1 at 0.90% is [-940.00 and -150.00] and contains the true value -844.81. The forecast interval of y_2 at 0.90% is [57.00, 174.00] and contains the true value 126.68. After adjusting for the mean and scale, we obtain forecasts of 46727.0 for Bitcoin and 3499.56 for Ethereum prices, which are off by 105 and 22 Dollars, respectively, outperforming a combined "no-change" forecast based on the previous day values.

The state variables

The Jordan decomposition is used to estimate the state variables $Z_{1,t}, Z_{2,t}$, which have financial interpretations in the cryptocurrency model. The noncausal state variables are the following combinations of the observed series:

$$\hat{Z}_{1,t} = -0.252Y_{1,t} + 0.240Y_{2,t}, \quad \hat{Z}_{2,t} = 0.252Y_{1,t} + 0.759Y_{2,t},$$

The noncausal state variable allocates positive weights to Bitcoin and Ethereum, like the Mega-Cap index. The causal state variable has a negative weight of Bitcoin. It represents a risk-neutral fund, i.e. a fund which is little sensitive to the changes in $Z_{2,t}$, and hedges against the common bubble effects. The two state variables are plotted in Figure 7.

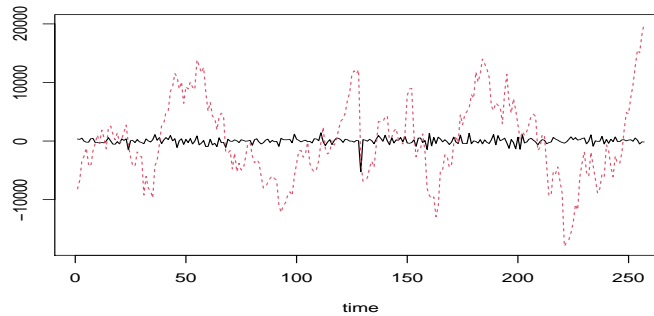


Figure 7: State Variables: black line: causal; red line: noncausal

We observe that the noncausal state variable captures the spikes and explosive patterns in cryptocurrency rates, while the causal state variable is much more stable.

Let us now compare the state variables with the factors obtained from a SVD (Singular Value Decomposition) of the marginal variance-covariance matrix $Var(Y_t)$. It is equivalent to consider the spectral decomposition of $Var(Y)$ and $Var(Z)$ as Y and Z satisfy a one-to-one linear relationship. It follows from (3.7)-(3.9) applied to the bivariate mixed VAR(1) model that:

$$Z_{1,t} = \sum_{h=0}^{\infty} [j_1^h a^1 \varepsilon_{t-h}], \quad Z_{2,t} = - \sum_{h=0}^{\infty} [(1/j_2)^{1+h} a^2 \varepsilon_{t+h+1}],$$

where a^1, a^2 are the rows of A^{-1} . We deduce that the matrix $Var(Z)$ is diagonal with

$$Var(Z_{1,t}) = \frac{1}{1 - j_1^2} a^1 \Sigma (a^1)', \quad Var(Z_{2,t}) = \frac{1}{j_2^2 - 1} a^2 \Sigma (a^2)'$$

In particular, the ordered eigenvectors are driven by either $Z_{1,t}, Z_{2,t}$ (resp. $Z_{2,t}, Z_{1,t}$) depending if $Var(Z_{1,t}) > Var(Z_{2,t})$ (resp. $Var(Z_{1,t}) < Var(Z_{2,t})$). The ordering can be reversed depending if the risk due to the explosive patterns is greater than the traditional risk measured by the variance of the causal component, or vice versa. In our example, we get $Var(Z_{2,t}) = 46904282.5$ and $Var(Z_{1,t}) = 347597.4$, as the variation of the explosive component is much higher.

Causal Analysis

i) Conditional Value-at-Risk of the noncausal component

The mixed VAR(1) model has a multiplicity of nonlinear autoregressive representations, and a multiplicity of state variables $Z_{1,t}, Z_{2,t}$ because of the multiplicity of Jordan forms. The former multiplicity gets reduced when the shocks on Z_1, Z_2 are ordered. This leads to a recursive form of the nonlinear autoregressive model:

$$Z_{2,t} = G_2(Z_{2,t-1}; v_{2,t}), \quad (6.1)$$

$$Z_{1,t} = G_{1|2}(Z_{2,t}, Z_{1,t-1}; v_{1,t}) \quad (6.2)$$

where function G_2 in $Z_{2,t} = G_2(Z_{2,t-1}; v_{2,t})$ is the inverse of function $v_{2,t} = \Phi^{-1}[F_2(Z_{2,t}|Z_{2,t-1})]$ in (4.3). By the Markov property of $(Z_{2,t})$ [see Corollary 4], $Z_{1,t-1}$ does not appear in equation (6.1).

For illustration, we focus on the CBS on the state variable Z_2 , which is a systemic factor of bubble risk, that is on the first equality of the recursive system.

It is easy to see that function $G_2(z, v_2)$ is the conditional Value-at-Risk (VaR) of Z_2 at level $\alpha = \Phi(v_2)$. This conditional VaR is easily estimated nonparametrically with a closed form expression of the estimator (see online Appendix D)

ii) Common Bubble Shock (CBS)

Since $\hat{G}(z, v_2)$ has a simple closed form expression, the equation (6.1) can be used to compare the future paths $Z_{2,T+1}^s, Z_{2,T+2}^s, \dots$ corresponding to a sequence of simulated innovations $(v_{T+1}^s, \dots, v_{T+H}^s)$ and to shocked at T+1 simulated shocks $(v_{T+1}^s + \delta, \dots, v_{T+H}^s)$.

Let us now consider the effect of a common bubble shock δ_2 performed at date T on $z_{2,T}$. Since the dynamic model is nonlinear, the IRF is nonlinear in δ_2 and in the value $y = (y_1, y_2)'$ of Y_T .

We observe that the impulse response functions are not symmetric in $\delta_2 = -2, -1, 0, 1, 2$

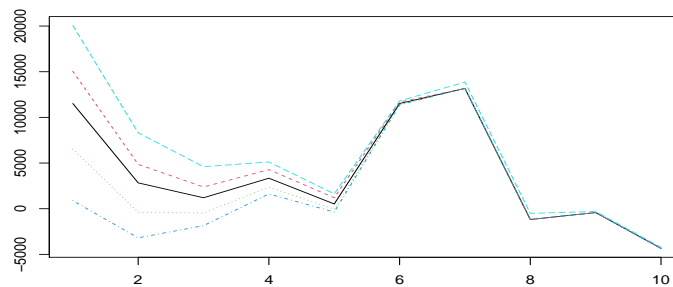


Figure 8: Impulse Response Functions: black line: baseline

7 Concluding Remarks

This paper considers the oos nonlinear forecasting and backcasting in a mixed VAR model. It introduces the closed-form expression of the causal (past-dependent) predictive distribution for forecasting a mixed (S)VAR model. As a post-estimation inference method, the confidence set of prediction set is introduced.

A definition of causal (past-dependent) nonlinear innovations for mixed VAR models is also given. Since the causal nonlinear innovations are not uniquely defined, their identification is examined.

The proposed approach is applied to the analysis of the joint dynamic of a bivariate series of cryptocurrency exchange rates. The state space representation reveals that the noncausal state variable captures the explosive patterns and can be interpreted as a crypto market portfolio, and that the causal state variable corresponds to a risk neutral fund. We also examined the impulse response functions associated with a common bubble shock (CBS).

REFERENCES

- Andrews, B, Davis, R. and J., Breidt (2006): "Maximum Likelihood Estimation of All-Pass Time Series Models", *Journal of Multivariate Analysis*, 97, 1638-1659.
- Axler, S., Bourdon, P. and W. Ramey (2001): "Harmonic Function Theory", 2nd Ed., *Graduate Texts in Mathematics*, Springer.
- Bec, F., Nielsen, H., and S., Saidi (2020): "Mixed Causal-Noncausal Autoregression: Bimodality Issues in Estimation and Unit Root Testing", *Oxford Bulletin of Economics and Statistics*, 82, 1413-1428.
- Bernoth, K., Herwartz, H., and L. Triener (2024): "The Impact of Global Risk and US Monetary Policy on US Dollar Exchange Rates with Excess Currency Returns", DP 2037, DIW, Berlin.
- Breidt, F., Davis, R., Lii, K., and M., Rosenblatt (1991) : "Maximum Likelihood Estimation for Noncausal Autoregressive Processes", *Journal of Multivariate Analysis*, 36, 175-198.

- Cambanis, S., and I., Fakhre-Zakeri (1994): "On Prediction of Heavy-Tailed Autoregressive Sequences Forward versus Reversed Time", *Theory of Probability and its Applications*, 39, 217-233.
- Cavaliere, G., Nielsen, H., and A., Rahbek (2020): "Bootstrapping Noncausal Autoregressions with Applications to Explosive Bubbles Modelling", *Journal of Business and Economic Statistics*, 38, 55-67.
- Comon, P. (1994): "Independent Component Analysis: A New Concept?", *Signal Process.*, 36, 287-314.
- Cordoni, F., and F., Corsi (2019): "Identification of Singular and Noisy Structural VAR Models: The Collapsing ICA Approach", D.P. University of Pisa.
- Cubadda, G., Hecq, A., and E., Voisin (2023): "Detecting Common Bubbles in Multivariate Mixed Causal-Noncausal Models", *Econometrics*, 11, 9.
- Davis, R., and L., Song (2020) : "Noncausal Vector AR Processes with Application to Economic Time Series", *Journal of Econometrics*, 216, 246-267.
- Fries, S., and J.M., Zakoian (2019): "Mixed Causal-Noncausal Autoregressive Processes", *Econometric Theory*, 35, 1234-1270.
- Gelfand, A., and A., Smith (1992): "Bayesian Statistics without Tears: A Sampling-Resampling Perspective", *Annals of Statistics*, 46, 84-88.
- Gonzalves, S., Herrera, A., Kilian, L., and E., Pesavento (2021): "Impulse Response Analysis for Structural Dynamic Models with Nonlinear Regressors", *Journal of Econometrics*, 225, 107-130.
- Gonzalves, S., Herrera, A., Kilian, L., and E., Pesavento (2022): "When Do State-Dependent Local Projections Work?", McGill U, working paper.
- Gourieroux, C., and A., Hencic (2015) : "Noncausal Autoregressive Model in Application to Bitcoin/USD Exchange Rates", *Econometrics of Risk, Studies in Computational Intelligence*, 583:17-40
- Gourieroux, C., and J., Jasiak (2005) : "Nonlinear Innovations and Impulse Responses with Application to VaR Sensitivity", *Annals of Economics and Statistics*, 78, 1-31.
- Gourieroux, C., and J., Jasiak (2016): "Filtering, Prediction, and Simulation Methods for Noncausal Processes", *Journal of Time Series Analysis*, 37, 405-430.
- Gourieroux, C., and J., Jasiak (2017): "Noncausal Vector Autoregressive Process: Representation, Identification and Semi-Parametric Estimation", *Journal of Econometrics*, 200, 118-134.
- Gourieroux, C., and J., Jasiak (2023): "Generalized Covariance Estimator", *Journal of Business and Economic Statistics*, 41, 1315 -1357.
- Gourieroux, C., Jasiak, J., and M., Tong (2021): "Convolution-Based Filtering and Forecasting: An Application to WTI Crude Oil Prices", *Journal of Forecasting*, 40, 1230-1244.
- Gourieroux, C., Monfort, A., and J.P., Renne (2017) : "Statistical Inference for Independent Component Analysis", *Application to Structural VAR Models*", *Journal of Econometrics*, 196, 111-126.
- Gourieroux, C., Monfort A., and J.P., Renne (2020): "Identification and Estimation in Nonfundamental Structural VARMA Models", *Review of Economic Studies*, 87, 1915-1953.
- Gourieroux, C., and J.M., Zakoian (2017) : "Local Explosion Modelling by Noncausal Process", *Journal of the Royal Statistical Society, B*, 79, 737-756.
- Guay, A. (2021): "Identification of Structural Vector Autoregressions Through Higher Unconditional Moments", *Journal of Econometrics*, 225, 27-45.
- Hall, M., and J., Jasiak (2024): "Modelling Common Bubbles in Cryptocurrency Prices", working paper at www.jjstats.com
- Hecq, A. , Lieb, L. and S., Telg (2016): "Identification of Mixed Causal-Noncausal Models in Finite Samples", *Annals of Economics and Statistics*, 123/124, 307-331.

- Imbens, G., and C., Manski (2004): "Confidence Intervals for Partially Identified Parameters", *Econometrica*, 72, 1845-1857.
- Keweloh, S. (2021): "A Generalized Method of Moments Estimator for Structural Vector Autoregressions Based on Higher Moments", *Journal of Business and Economic Statistics*, 39, 772-782.
- Koop, G., Pesaran, H., and S., Potter (1996): "Impulse Response Analysis in Nonlinear Multivariate Models", *Journal of Econometrics*, 74, 119-147.
- Lanne, M., and J., Luoto (2016): "Noncausal Bayesian Vector Autoregression", *Journal of Applied Econometrics*, 31, 1392-1406.
- Lanne, M., and P., Saikkonen (2008): "Modelling Expectations with Noncausal Autoregressions", MPRA paper 8411.
- Lanne, M., and P., Saikkonen (2011a) : "Noncausal Autoregressions for Economic Time Series", *Journal of Time Series Econometrics*, 3, 1-39.
- Lanne, M., and P., Saikkonen (2011b) : "GMM Estimators with Non-Causal Instruments", *Oxford Bulletin of Economics and Statistics*, 71, 581-591.
- Lanne, M., and P., Saikkonen (2013) : "Noncausal Vector Autoregression", *Econometric Theory*, 29, 447-481.
- Lutkepohl, H. (1990): "Asymptotic Distribution of Impulse Response Functions and Forecast Error Variance Decomposition of Vector Autoregressive Models", *Review of Economics and Statistics*, 72, 116-125.
- Nyberg, H., and P., Saikkonen (2014): "Forecasting with a Noncausal VAR Model", *Computational Statistics and Data Analysis*, 76, 536-555.
- Perko, L. (2001): "Differential Equations and Dynamical Systems", Springer, New York.
- Potter, S. (2000): "Nonlinear Impulse Response Functions", *Journal of Economic Dynamics and Control*, 24, 1425-1426.
- Rosenblatt, M. (2012) : "Gaussian and Non-Gaussian Linear Time Series and Random Fields", Springer Verlag.
- Starck, V. (2023): "Estimation of Independent Component Analysis Systems", Working Paper, Brown University.
- Swensen, A. (2022): "On Causal and Non-Causal Cointegrated Vector Autoregressive Time Series", *Journal of Time Series Analysis*, 42, 178-196.
- Tanner, M. (1993): "Tools for Statistical Inference", Springer Series in Statistics, 2nd edition, Springer, New York.
- Twumasi, C. and J. Twumasi (2022): "Machine Learning Algorithms for Forecasting and Back-casting Blood Demand Data with Missing Values and Outliers: A Study of Tema General Hospital of Ghana", *International Journal of Forecasting*, 38, 1258-1277.
- Velasco, C. (2023): "Identification and Estimation of Structural VARMA Models Using Higher Order Dynamics", *Journal of Business and Economic Statistics*, 41, 819-832.
- Velasco, C., and I., Lobato (2018): "Frequency Domain Minimum Distance Inference for Possibly Noninvertible and Noncausal ARMA Models", *Annals of Statistics*, 46, 555-579.

APPENDIX A
APPENDIX A.1
Proof of Proposition 1

The proof follows along the same lines as in Gouriéroux, Jasiak (2016), (2017), with an additional attention given to the information sets and the use of Jacobian formulas on manifolds. The derivation is greatly simplified for special cases of VAR(1) processes with a multiplicative representation [Lanne, Saikkonen (2013)].

1) Let us consider the information set:

$$I_{T+1} = (Y_1, \dots, Y_T, Y_{T+1}).$$

This set is equivalent to the set generated by $(Z_1, Z_2, \dots, Z_{T+1})$ and the set generated by $(Z_{1,2}, \eta_3, \eta_4, \dots, \eta_T, \eta_{T+1})$ by using the recursive equations (3.8). Since $(\eta_{1,T+1}, Z_{2,T}, Z_{2,T+1})$ is independent of $\underline{\varepsilon}_T$, we see that the conditional density $l(\eta_{1,T+1}, Z_{2,T}, Z_{2,T+1} | \underline{\varepsilon}_T) = l(\eta_{1,T+1}, Z_{2,T}, Z_{2,T+1})$ is equal to the marginal density.

It follows that the conditional density is:

$$l(\eta_{1,T+1}, Z_{2,T+1} | Z_{2,T}, \underline{\varepsilon}_T) = l(\eta_{1,T+1}, Z_{2,T+1} | I_T) = l(\eta_{1,T+1}, Z_{2,T+1} | Z_{2,T}). \quad (\text{a.1})$$

The last conditional density needs to be rewritten with a conditioning variable being the future Z_2 . From the Bayes theorem, it follows that:

$$l(\eta_{1,T+1}, Z_{2,T+1} | I_T) = \frac{l_2(Z_{2,T+1})}{l_2(Z_{2,T})} l(\eta_{1,T+1}, Z_{2,T} | Z_{2,T+1}), \quad (\text{a.2})$$

where l_2 is the marginal density of $Z_{2,t}$.

2) Let us now consider the vector $\eta_t = A^{-1} \begin{pmatrix} \varepsilon_t \\ 0 \end{pmatrix}$. This random vector takes values on the subspace $E = A^{-1}(\mathbb{R}^m \times 0^{n-m})$. Its distribution admits a density $g_\eta(\eta_1, \eta_2)$ with respect to the Lebesgue measure on subspace E . Moreover, we have:

$$\eta_{T+1} = \begin{pmatrix} \eta_{1,T+1} \\ Z_{2,T+1} - J_2 Z_{2,T} \end{pmatrix} = \begin{pmatrix} Id & 0 \\ 0 & -J_2 \end{pmatrix} \begin{pmatrix} \eta_{1,T+1} \\ Z_{2,T} \end{pmatrix} + \begin{pmatrix} 0 \\ Z_{2,T+1} \end{pmatrix}. \quad (\text{a.3})$$

Then, conditional on $Z_{2,T+1}$, vector $\begin{pmatrix} \eta_{1,T+1} \\ Z_{2,T} \end{pmatrix}$ takes values in the affine subspace $F = \begin{pmatrix} Id & 0 \\ 0 & -J_2 \end{pmatrix}^{-1} \left[E - \begin{pmatrix} 0 \\ Z_{2,T+1} \end{pmatrix} \right]$ with a density with respect to the Lebesgue measure on F . Since the transformation from η_{T+1} to $\begin{pmatrix} \eta_{1,T+1} \\ Z_{2,T} \end{pmatrix}$ is linear affine invertible, we can apply the Jacobian formula to get:

$$l(\eta_{1,T+1}, Z_{2,T} | Z_{2,T+1}) = |\det J_2| g_\eta(\eta_{1,T+1}, Z_{2,T+1} - J_2 Z_{2,T}). \quad (\text{a.4})$$

Then from (a.2), (a.4) and $Z_{1,T+1} = J_1 Z_{1,T} + \eta_{1,T+1}$, it follows that:

$$l(Z_{1,T+1}, Z_{2,T+1} | I_T) = \frac{l_2(Z_{2,T+1})}{l_2(Z_{2,T})} |\det J_2| g_\eta(Z_{1,T+1} - J_1 Z_{1,T}, Z_{2,T+1} - J_2 Z_{2,T}). \quad (\text{a.5})$$

Let us now derive the predictive density of Y_{T+1} given I_T . We get a succession of affine transformations of variables with values in different affine subspaces (depending on the conditioning set) along the following scheme:

$$\begin{pmatrix} \varepsilon_{T+1} \\ 0 \end{pmatrix} \xrightarrow{A^{-1}} \eta_{T+1} \xrightarrow{Id} Z_{T+1} \xrightarrow{A} \begin{pmatrix} Y_{T+1} \\ \tilde{Y}_T \end{pmatrix}.$$

(given Z_T) (given \tilde{Y}_T)

Then, we can apply three times the Jacobian formula on manifolds. Since $|\det A^{-1}| |\det A| = \frac{|\det A|}{|\det A|} = 1$, the Jacobians cancel out and the predictive density becomes:

$$l(y|\underline{Y}_T) = \frac{l_2 \left[A^2 \begin{pmatrix} y \\ \tilde{Y}_T \end{pmatrix} \right]}{l_2 \left[A^2 \begin{pmatrix} Y_T \\ \tilde{Y}_{T-1} \end{pmatrix} \right]} |\det J_2| g(y - \Phi_1 Y_T - \dots - \Phi_p Y_{T-p+1}),$$

which yields the formula in Proposition 1.

In addition, from (a.5) we derive the predictive density of Z_{T+1} given \underline{Z}_T as:

$$l(Z_{T+1}|\underline{Z}_T) = \frac{l_2(Z_{2,T+1})}{l_2(Z_{2,T})} |\det J_2| |\det A| g \left(A \begin{bmatrix} Z_{1,T+1} - J_1 Z_{1,T} \\ Z_{2,T+1} - J_2 Z_{2,T} \end{bmatrix} \right). \quad (\text{a.6})$$

The predictive density of Z_{T+1} depends on the choice of the state space representation, whereas the predictive density of Y_T does not.

Proof of Corollary 2

To keep the notation simple, let us assume a mixed VAR(1) model. Then, from Corollary 1, it follows that (Y_t) as well as (Z_t) are Markov processes of order 1 in both calendar and reverse time. The distribution of process (Z_t) is characterized by the pairwise distribution of (Z_{t-1}, Z_t) .

From the proof of Proposition 1, it follows that this joint distribution is:

$$l(z_{t-1}, z_t) = l_1(z_{1,t-1}) l_2(z_{2,t}) |\det J_2| g_\eta(z_{1,t} - J_1 z_{1,t-1}, z_{2,t} - J_2 z_{2,t-1}).$$

Then, the conditional distribution of Z_{t-1} given $Z_t = z_t$ is:

$$\begin{aligned} l(z_{t-1}|z_t) &= l(z_{t-1}, z_t) / l(z_t) \\ &= l(z_{t-1}, z_t) / [l_1(z_{1,t}) l_2(z_{2,t})], \text{ because } Z_{1,t} \text{ and } Z_{2,t} \text{ are independent,} \\ &= \frac{l_1(z_{1,t-1})}{l_1(z_{1,t})} |\det J_2| g_\eta(z_{1,t} - J_1 z_{1,t-1}, z_{2,t} - J_2 z_{2,t-1}). \end{aligned}$$

The result in Corollary 2 follows by applying the transformations: $Y_t = AZ_t$, $\varepsilon_t = A\eta_t$.

APPENDIX A.2 The Multiplicative Causal-Noncausal Model

The multiplicative causal-noncausal model is:

$$\Phi(L)\Psi(L^{-1})Y_t = \varepsilon_t^*,$$

where both autoregressive polynomials have roots outside the unit circle and i.i.d. errors ε_t^* [Lanne, Luoto, Saikkonen (2012), Lanne, Saikkonen (2013) and Nyberg, Saikkonen (2014)]. While for

univariate time series the multiplicative representation is equivalent to the general AR(p) model, it is not the case in the multivariate framework (except for the VAR(1) process).

As pointed out in Davis, Song (2020), p. 247, this decomposition implies restrictions on the autoregressive coefficients Φ_1, \dots, Φ_p of the past-dependent representation.

Moreover, it is not compatible in general with the VAR specification (2.1). To illustrate this problem, let us consider the multiplicative bivariate model:

$$\begin{pmatrix} 1 - \phi L & 0 \\ 0 & 1 \end{pmatrix} \begin{pmatrix} 1 & 0 \\ 0 & 1 - \psi L^{-1} \end{pmatrix} Y_t = \varepsilon_t^*.$$

It follows that:

$$\begin{aligned} Y_{1,t} - \phi Y_{1,t-1} &= \varepsilon_{1,t}^*, \\ Y_{2,t} - \psi Y_{2,t+1} &= \varepsilon_{2,t}^*, \end{aligned}$$

or equivalently, if $\Psi \neq 0$,

$$\begin{aligned} Y_{1,t} - \phi Y_{1,t-1} &= \varepsilon_{1,t}^*, \\ Y_{2,t} - \frac{1}{\psi} Y_{2,t-1} &= -\frac{1}{\psi} \varepsilon_{2,t-1}^*, \\ \iff Y_t &= \begin{pmatrix} \phi & 0 \\ 0 & \frac{1}{\psi} \end{pmatrix} Y_{t-1} + \varepsilon_t, \end{aligned}$$

where $\varepsilon_t = \begin{pmatrix} \varepsilon_{1,t} \\ \varepsilon_{2,t} \end{pmatrix}$ with $\varepsilon_{1,t} = \varepsilon_{1,t}^*$ and $\varepsilon_{2,t} = -\frac{1}{\psi} \varepsilon_{2,t-1}^*$.

We observe that, if $\varepsilon_{1,t}^*, \varepsilon_{2,t}^*$ are contemporaneously correlated, then $\varepsilon_{1,t}$ and $\varepsilon_{2,t+1}$ are correlated too. Therefore the condition of i.i.d. errors in the VAR model (2.1) cannot be satisfied.

This major difficulty is a consequence of a different normalization. For example, if $\Phi(L) = Id - \Phi L$ and $\Psi(L^{-1}) = Id - \Psi L^{-1}$, then the multiplicative model is such that:

$$\Phi(L)\Psi(L^{-1})Y_t = -\Psi Y_{t+1} + (Id + \Phi\Psi)Y_t - \Phi Y_{t-1} = \varepsilon_t^*,$$

which cannot be transformed into:

$$Y_t = \Phi_1 Y_{t-1} + \Phi_2 Y_{t-2} + \varepsilon_t,$$

with i.i.d. errors, if matrix Ψ is not invertible.

APPENDIX A.3

Identification of Nonlinear Causal Innovations

a) Existence of nonlinear causal autoregressive representation

For ease of exposition, let us consider a bivariate Markov process. By analogy to the recursive causal approach for defining the shocks, we start from the first component.

i) Let $F_1[y_1|Y_{T-1}]$ denote the conditional c.d.f. of $Y_{1,T}$ given Y_{T-1} and define:

$$v_{1,T} = F_1[Y_{1,T}|Y_{T-1}], \quad \forall T. \quad (\text{a.7})$$

Then, $v_{1,T}$ follows a uniform distribution $U_{[0,1]}$ for any Y_{T-1} . In particular, $v_{1,T}$ is independent of Y_{T-1} .

ii) Let $F_2[y_2|Y_{1,T}, Y_{T-1}]$ denote the conditional c.d.f. of $Y_{2,T}$ given $Y_{1,T}, Y_{T-1}$, and define:

$$v_{2,T} = F_2[Y_{2,T}|Y_{1,T}, Y_{T-1}], \quad \forall T. \quad (\text{a.8})$$

It follows that $v_{2,T}$ follows a uniform distribution on $[0,1]$, for any $Y_{1,T}, Y_{T-1}$, or equivalently for any $v_{1,T}, Y_{T-1}$. Therefore, $v_{2,T}$ is independent of $v_{1,T}, Y_{T-1}$.

iii) By inverting equations (a.6)-(a.7), we obtain a nonlinear autoregressive representation: $Y_T = a(Y_{T-1}, v_T)$, where the v_T 's are i.i.d. such that $(v_{1,T}), (v_{2,T})$ are independent.

Alternatively, one can use the ordering: $Y_{2,T}$ followed by $Y_{1,T}$ given $Y_{2,T}$. More generally, for any invertible nonlinear transformation $Y_T^* = c(Y_T)$, the above approach can be applied first to $Y_{1,T}^*$ and next to $Y_{2,T}^*$ conditional on $Y_{1,T}^*$.

Therefore any Markov process can be written as a nonlinear causal autoregressive process and the above discussion shows that this autoregressive representation is not unique.

b) Identification of the nonlinear causal autoregressive representation

It is equivalent to consider the identification of function a or the identification of nonlinear innovations. Let us now describe in detail all the nonlinear causal innovation identification issues. First, we can assume that $v_{1,T}, v_{2,T}$ are i.i.d and independent of one another with uniform distributions on $[0,1]$. We need to find out if there exists another pair of variables $w_{1,T}, w_{2,T}$, which are independent and uniformly distributed such that:

$$a(Y_{T-1}, w_T) = a(Y_{T-1}, v_T), \quad \forall Y_{T-1},$$

or, equivalently, a pair of variables w_T that satisfy a (nonlinear) one-to-one relationship with v_T . Let $w = b(v)$ denote this relationship. We have the following Lemma:

Lemma A.1:

Let us assume that b is continuous, twice differentiable and that the Jacobian matrix $\partial b(v)/\partial v'$ has distinct eigenvalues. Then, the components of b are harmonic functions, that is:

$$\frac{\partial^2 b_j(v)}{\partial v_1^2} + \frac{\partial^2 b_j(v)}{\partial v_2^2} = 0, \quad j = 1, 2.$$

Proof:

i) We can apply the Jacobian formula to get the density of w given the density of v . Since both joint densities are uniform, it follows that $|\det \frac{\partial b(v)}{\partial v'}| = 1, \forall v \in [0, 1]^2$.

ii) Let us consider the eigenvalues $\lambda_1(v), \lambda_2(v)$ of the Jacobian matrix $\frac{\partial b(v)}{\partial v'}$. The eigenvalues are continuous functions of this matrix, and therefore continuous functions of v (whenever these eigenvalues are different). Then, two cases can be distinguished:

case 1: The eigenvalues are real.

case 2: The eigenvalues are complex conjugates.

iii) In case 1, we have $\lambda_2(v) = 1/\lambda_1(v)$ (or $-1/\lambda_1(v)$), where $\lambda_1(v)$ is less or equal to 1 in absolute value for any v , and then $\lambda_2(v)$ is larger than or equal to 1 in absolute value for any v . Since $b(v) \in [0, 1]^2$ for any $v \in [0, 1]^2$, it follows that $\lambda_2(v)$ cannot be explosive.

iv) Therefore case 2 of complex conjugate roots is the only relevant one. Let us consider the case $\det \frac{\partial b(v)}{\partial v'} = 1, \forall v \in [0, 1]^2$ (the analysis of $\det \frac{\partial b(v)}{\partial v'} = -1$ is similar). Then, the Jacobian matrix is a rotation matrix:

$$\frac{\partial b(v)}{\partial v'} = \begin{pmatrix} \frac{\partial b_1(v)}{\partial v_1} & \frac{\partial a_1(v)}{\partial v_2} \\ \frac{\partial b_2(v)}{\partial v_1} & \frac{\partial b_2(v)}{\partial v_2} \end{pmatrix} \equiv \begin{pmatrix} \cos \theta(v) & -\sin \theta(v) \\ \sin \theta(v) & \cos \theta(v) \end{pmatrix}.$$

Thus the standard identification issue known in the linear SVAR model that is up to a given rotation matrix is replaced by the analogue in which the rotation matrix is local and depends on v . We deduce that:

$$\begin{aligned} \frac{\partial b_1(v)}{\partial v_1} &= \frac{\partial b_2(v)}{\partial v_2}, \\ \frac{\partial b_1(v)}{\partial v_2} &= -\frac{\partial b_2(v)}{\partial v_1}. \end{aligned} \tag{a.9}$$

Let us differentiate the first equation with respect to v_1 and the second one with respect to v_2 . We get:

$$\frac{\partial^2 b_1(v)}{\partial v_1^2} = \frac{\partial^2 b_2(v)}{\partial v_1 \partial v_2} \quad \text{and} \quad \frac{\partial^2 b_1(v)}{\partial v_2^2} = -\frac{\partial^2 b_2(v)}{\partial v_1 \partial v_2}, \tag{a.10}$$

and by adding these equalities:

$$\frac{\partial^2 b_1(v)}{\partial v_1^2} + \frac{\partial^2 b_1(v)}{\partial v_2^2} = 0. \tag{a.11}$$

Therefore b_1 is a harmonic function that satisfies the Laplace equation (a.10). Similarly, b_2 is also a harmonic function. QED

Harmonic functions are regular functions: they are infinitely differentiable and have series representations that can be differentiated term by term [Axler et al. (2001)]:

$$\begin{aligned} b_1(v) &= \sum_{h=0}^{\infty} \sum_{k=0}^{\infty} (b_{1hk} v_1^k v_2^h), \\ b_2(v) &= \sum_{h=0}^{\infty} \sum_{k=0}^{\infty} (b_{2hk} v_1^k v_2^h). \end{aligned} \tag{a.12}$$

Moreover, these series representations are unique. Then, we can apply the conditions (a.8) to these expansions to derive the constraints on the series coefficients and the link between functions b_1 and b_2 .

Let us define:

$$\frac{\partial b_1(v)}{\partial v_1} = \frac{\partial b_2(v)}{\partial v_2} \equiv \sum_{h=0}^{\infty} \sum_{k=0}^{\infty} (c_{hk} v_1^h v_2^k).$$

Then, by integration, we get:

$$\begin{aligned} b_1(v) &\equiv \sum_{h=0}^{\infty} \sum_{k=0}^{\infty} [c_{hk} \frac{v_1^{h+1}}{h+1} v_2^k] + \sum_{k=0}^{\infty} d_{1k} v_2^k, \\ b_2(v) &\equiv \sum_{h=0}^{\infty} \sum_{k=0}^{\infty} [c_{hk} v_1^h \frac{v_2^{k+1}}{k+1}] + \sum_{h=0}^{\infty} d_{2h} v_1^h, \end{aligned}$$

where the second sums on the right hand sides are the integration "constants". Equivalently, we have:

$$\begin{aligned} b_1(v) &\equiv \sum_{k=0}^{\infty} d_{1k} v_2^k + \sum_{h=1}^{\infty} \sum_{k=0}^{\infty} [c_{h-1,k} \frac{v_1^h}{h} v_2^k], \\ b_2(v) &\equiv \sum_{h=0}^{\infty} d_{2h} v_1^h + \sum_{h=0}^{\infty} \sum_{k=1}^{\infty} [c_{h,k-1} v_1^h \frac{v_2^k}{k}]. \end{aligned}$$

Let us now write the second equality in (a.8), i.e.

$$\frac{\partial b_1(v)}{\partial v_2} = -\frac{\partial b_2(v)}{\partial v_1}.$$

This yields:

$$\begin{aligned} \frac{k+1}{h} c_{h-1,k+1} &= -\frac{h+1}{k} c_{h+1,k-1}, \quad h \geq 1, k \geq 1, \\ \frac{1}{h} c_{h-1,1} &= -(h+1) d_{2,h+1} \quad h \geq 1, \\ \frac{1}{h} c_{1,k-1} &= -(k+1) d_{1,k+1} \quad k \geq 1, \\ d_{11} &= -d_{21}. \end{aligned} \tag{a.13}$$

The set of restrictions (a.12) provides information on the dimension of underidentification. As the dimension concerns functional spaces, we describe it from the series expansions (a.11) and the number of independent parameters $b_{1,h,k}, b_{2,h,k}$ with $h+k \leq m$. This number is equal to $(m+1)(m+2)/2$.

Proposition A.2

The space of parameters $(b_{1,h,k}, b_{2,h,k}, h+k \leq m)$ is of dimension $2m$.

Proof:

Let us consider an alternative parametrization of (a.12) with parameters $c_{h,k}, d_{1,h}, d_{2,h}$. The parameters $b_{1,h,k}, b_{2,h,k}$ with $h+k = j$ are linear functions of parameters $c_{h,k}, h+k = j+1, d_{1,j+1}, d_{2,j+1}$. Then the result follows from restrictions (a.12).

QED

Other identification issues can arise if transformation b is not assumed twice continuously differentiable. Let us consider the first component v_1 that follows the uniform distribution on $[0, 1]$ and introduce two intervals $[0, c]$ and $[1 - c, 1]$ with $c < 0.5$. Then, the variable w_1 defined by:

$$w_1 = \begin{cases} v_1, & \text{if } v_1 \in (c, 1 - c), \\ 2v_1 - 1, & \text{if } v_1 \in (0, c) \cup (1 - c, 1), \end{cases}$$

also follows the uniform distribution and, similarly to v_1 , variable w_1 is independent of $v_2 = w_2$.

Note that this transformation is not monotonous. Therefore, the size δ of a shock to v_1 is difficult to interpret in terms of a magnitude of a shock to w_1 .

We conclude that, in a nonlinear dynamic framework, the assumption of independence between the components of v_t is insufficient to identify the structural innovations to be shocked.